TURUN YLIOPISTO

Microplastics in Varved Sediments of Haverö Sedimentary Basin

Quaternary geology

Master's thesis

Credits: 30

Author:

Henri Heikkinen

29.05.2026

Turku

Master's thesis

Subject: Quaternary geology
Author: Henri Heikkinen
Title: Microplastics in varved sediments of Haverö sedimentary basin
Supervisor: Associate professor, Saija Saarni
Number of pages: 66 pages
Päivämäärä: 29.5.2026

The exponential growth of plastic production during the past century has increased the amount of microplastics that accumulate in marine ecosystems and in sediments, yet high-resolution historical accumulation rates remain poorly resolved. This study presents a new methodological approach to investigating microplastic abundance, polymer types, and concentrations in annually laminated sediments from an enclosed, hypoxic basin of Haverö located in the Turku Archipelago Sea, Finland. The use of varved sediments in the study of microplastics can provide a temporal insight into microplastic accumulation on a year-to-year basis.

A sediment core spanning 60 years (1964-2024) was retrieved and later subsampled. LOI and MS values were measured for each varve year, also reflecting compositional variations in the varve structure. Due to the time-intensive nature of MP extraction, 16 of the most recent varves (2009-2024) underwent heavy liquid separation and enzymatic purification stages to separate the sediment from the MPs. After purification and filtering 16 samples were analysed for MP identification using FTIR spectroscopy and the FTIR-data processed through siMPle software. A total of 258 MPs were found from 256.65 g of dry weight sediment. PE and PP were the most abundant polymer types found in the samples. Observed MP concentrations in the Haverö basin from 16 varved sediment samples were found to be 1.006 MPs/g. The abundance and concentration of MPs was likely lower due to the samples being saturated with biogenic chitin shells which were filtered through a 100 µm mesh prior to FTIR. This excluded the presence of MPs <100 µm found in the samples.

This study demonstrates the feasibility of separating MPs from varved sediments and lends temporal insight into variation of MP abundances, concentrations, and polymer types for each varve year. This study also serves as an important framework for future research on microplastics using varved sediments and highlights what can be improved in the methodology.

Key words: Varved sediments, microplastics, FTIR, enzyme treatment, Baltic Sea, paleolimnology

Pro gradu -tutkielma

Oppiaine: Maaperägeologia
Tekijä: Henri Heikkinen
Otsikko: Mikromuovit Haverön lustosedimenteissä
Ohjaaja: Apulaisprofessori, Saija Saarni
Sivumäärä: 66 sivua
Päivämäärä: 29.5.2026

Muovituotannon eksponentiaalinen kasvu viime vuosisadan aikana on lisännyt meriekosysteemeihin ja sedimentteihin kertyvien mikromuovien määrää, mutta niiden historialliset kertymänopeudet korkealla ajallisella resoluutiolla tunnetaan edelleen heikosti. Tässä tutkimuksessa esitetään uusi menetelmällinen lähestymistapa mikromuovien määrän, polymeerien ja pitoisuuksien tutkimiseen vuosikerrallisista sedimenteistä Saaristomerellä sijaitsevasta Haverön altaasta, jossa vallitsee happikato. Lustosedimenttien käyttö mikromuovitutkimuksessa voi tuoda tarkkaa ajallista tietoa mikromuovien kertymisestä vuosi vuodelta.

60 vuotta (1964–2024) kattava sedimenttikairanäyte otettiin tutkimusalueelta ja jaettiin myöhemmin osanäytteisiin. Hehkutushäviö ja magneettisen suskeptibiliteetin arvot mitattiin jokaiselta lustovuodelta, mikä myös heijastaa sedimentin lustorakennetta. 16 viimeisintä lustoa (2009–2024) käsiteltiin raskasneste-erotuksella ja entsymaattisella käsittelyllä sedimentin erottamiseksi mikromuoveista. Entsyymikäsittelyn ja suodatuksen jälkeen samat 16 näytettä analysoitiin mikromuovien tunnistamiseksi käyttäen FTIR-ohjelmistoa ja tulokset analysoitiin SiMPle:llä

Yhteensä 258 mikromuovia löydettiin 256.65 grammasta kuivapainoista sedimenttiä. PE ja PP olivat näytteissä yleisimmät havaitut polymeerityypit. Haverön altaan 16 näytteestä havaituksi mikromuovipitoisuudeksi saatiin 1.006 MPs/g. Mikromuovien runsaus ja pitoisuus olivat todennäköisesti todellisuudessa suurempia, koska näytteet sisälsivät runsaasti biogeenisiä kitiinikuoria, jotka suodatettiin 100 µm:n verkon läpi ennen FTIR-analyysia. Tämän avulla saatiin suljettua pois alle 100 µm:n kokoiset mikromuovit näytteistä.

Tutkimus osoittaa, että mikromuovien erottaminen lustosedimenteistä on toteutettavissa, ja tarjoaa ajallista tietoa mikromuovien määristä, pitoisuuksista ja polymeerityypeistä jokaiselta lustovuodelta. Tutkimus toimii myös tärkeänä pohjana tulevalle lustosedimenttejä hyödyntävälle mikromuovitutkimukselle sekä menetelmän kehittämismahdollisuuksien arvioinnille.

Avainsanat: Lustosedimentti, mikromuovit, FTIR, entsyymikäsittely, Itämeri, paleolimnologia

Table of contents

Abbreviations and glossary

BEPP = basic enzymatic purification protocol

CE = Current Era

CO_2-eq = Carbon dioxide equivalent

DW sediment = Dry weight of the sediment after drying in 105°C for 24h

EEA = European Environment Agency

FTIR = Fourier transform-infrared spectroscopy

HDPE = High density polyethylene

ImageJ = Image Processing and Analysis in Java -software

LOI = Loss-on-ignition

LST = Lithium polytungstate

MP = Microplastic, 1 µm to 5mm in size

MS = Magnetic susceptibility

Nanoplastic = Plastic particles smaller than 1 µm in size.

NOAA = National Oceanic and Atmospheric Administration

PA = Polyamide

PE = Polyethylene

PET = Polyethylene terephthalate

PP = Polypropylene

PS = Polystyrene

PVC = Polyvinyl chloride

SIB Labs = SIB Labs, Science – Innovation – Business, key operations are focusing on the transfer of scientific expertise and service production related to special equipment to its customers in research, business, and education.

SiMPle = Systematic Identification of MicroPlastics in the Environment. Developed by Aalborg University, Denmark and Alfred Wegener Institute, Germany.

UHQ water = Ultra-high purity water

The use of AI in master's thesis writing

Artificial intelligence tools, including ChatGPT and Google Gemini, were used sparingly during the preparation of this master's thesis. ChatGPT was used to improve the conciseness of the abstract so that it would fit on a single page. Google Gemini was used to identify the appropriate Microsoft Excel formula for generating Figure 12.

1. Introduction

Global plastic production has increased dramatically over the past century, rising from approximately 0.5 million tonnes in 1950 to over 260 million tonnes in 2009 and exceeding 367 million tonnes by 2020 (Ashrafy et al. 2023; Thompson et al. 2009). Plastics are used in a wide variety of applications nowadays ranging from toys, aircraft, appliances, medical equipment, clothes, and cars (Thompson et al. 2009; Van Cauwenberghe et al. 2015). Because of the wide-ranging versatility of plastics, their resistance to degradation, and their low manufacturing costs, massive amounts of these plastics eventually end up in landfills where they take centuries to degrade or in our water ecosystems if improperly disposed (Cole et al. 2011). Plastics alongside microplastics pose health risks for aquatic organisms when ingested. These detrimental health effects include but are not limited to immune system disturbances, hormone dysregulation, and reproductive issues (Cole et al. 2011; Thompson et al. 2009; Van Cauwenberghe et al. 2015).

The focus of this research was to explore the plastics that end up in marine ecosystems, and a particular focus will be placed on microplastics (1 μm to 5 mm in diameter). The study of microplastics is still in its preliminary stages. This study provides an insight into the amounts and varieties of microplastics that exist in our marine ecosystems, and to provide new temporal perspective into how these microplastics have sedimented during a 16-year period using varve chronology in Haverö sedimentary basin, located in Southwest Finland. Coastal systems are particularly vulnerable to microplastic pollution given their proximity to human settlements, and coastal communities rely on a wide range of resources in the aquatic zone for their subsistence (Ashrafy et al. 2023; Van Cauwenberghe et al. 2015). The sediment core was taken from a location next to Haverö island where the circumstances are optimal for varve formation in a water depth of ~20 meters. Downcore counting of laminations in varved sediments offers a direct and incremental dating technique for high-resolution climatic and environmental archives with at least annual and often even seasonal resolution (Zolitschka et al. 2015). The varved sediments found in Haverö sediment basin thus serve as an archive into the past and because the plastics are relatively persistent when buried in sediments.

2. Background

According to Chalmin's (2019) publication, plastics were first introduced back in 1833 in the form of nitrocellulose which was later industrialized by Hyatt brothers in 1868 to create billiard balls. However, the first fully synthetic plastic came in the form of bakelite, created by Leo Hendrik Baekeland in 1907 (Plastics Europe 2021). For example, early telephones were made from this bakelite material (Plastics Europe 2021). However, it was not until the First and Second World Wars that global plastic production started to increase markedly (Chalmin 2019). The development of plastics advanced rapidly as a result of the introduction of cellophane in 1913, polyvinyl chloride (PVC) in 1927, polystyrene (PS) in 1938 and polyethylene (PE) in 1942 which are some of the most prevalent types of plastics in the present day still being produced (Abel et al. 2023; Chalmin 2019; Plastics Europe 2021). In 2024, 220 million tons of plastic waste was generated which translates to an average of 28 kg of plastic per person (Safe Food Advocacy Europe 2024). According to the European Environmental Agency (2024), over half of all produced plastic has been produced after the year 2000, which is a drastic increase from the early days of plastic production. Additionally, according to the EEA (2024), only 9% of all produced plastic has been recycled and 12% of produced plastic has been incinerated. The remaining plastics have ended up in landfills or have been discarded into the environment, where they undergo further degradation but do not decompose.

Plastics are made from coal, natural gas, salt, and, most importantly, crude oil. (EEA 2024). The production of plastics begins with the distillation of crude oil in an oil refinery. This separates the heavy crude oil into groups of lighter components, called fractions. Each fraction is a mixture of hydrocarbon chains. One of these fractions, naphtha is an important ingredient in plastic production (EEA 2024). Plastics are therefore mostly synthetic and originate from primarily fossil fuels and need to go through multiple industrial processes for plastics to be formed (EEA 2024).

Data from the EEA Greenhouse Gas Inventory shows that annual greenhouse gas emissions related to plastic production in the EU amount to approximately 13.4 million tonnes of CO_2. When considering the whole lifecycle of plastics, this amount has been estimated to be 132 million tonnes of CO_2-eq in EU in 2018 (EEA 2021). Converting these polymers to plastic components and products accounts for an additional 46 million tonnes.

Plastic packaging amounts to 40% all plastic that's being produced (EEA 2021). Plastics are preferred in many industries because they're durable, lightweight, and cost-effective to produce. Because of these traits, plastics have become ubiquitous virtually everywhere on Earth (EEA 2021). However, since such vast amounts of plastic is produced every year, not all of it can be re-used (EEA 2021).

Several approaches are currently available to support a circular economy for plastics. One challenge in plastic recycling is the existence of multiple plastic types with different polymer structures (EEA 2021). Some distinct types of plastics and their use cases are for example, PET used in bottles, HDPE used in shampoo bottles and polypropylene (PP) used in single-use plastic cups (EEA 2021). The EEA (2021) report presents the main issues that are impeding with the transition to a more circular model for plastic use, as opposed to the linear one currently being engaged. Plastics are designed to be short-lived and readily discarded after they've fulfilled their purpose for example as packaging material (Figure 1). This contributes to increased CO_2 emissions, as plastics are incinerated, during which the extraction of oil and gas for plastic production, greenhouse gases and pollutants are emitted to the atmosphere, and large volumes of wastewater containing dispersed oil, hazardous substances and other toxic chemicals are leaked into the environment (Figure 1).

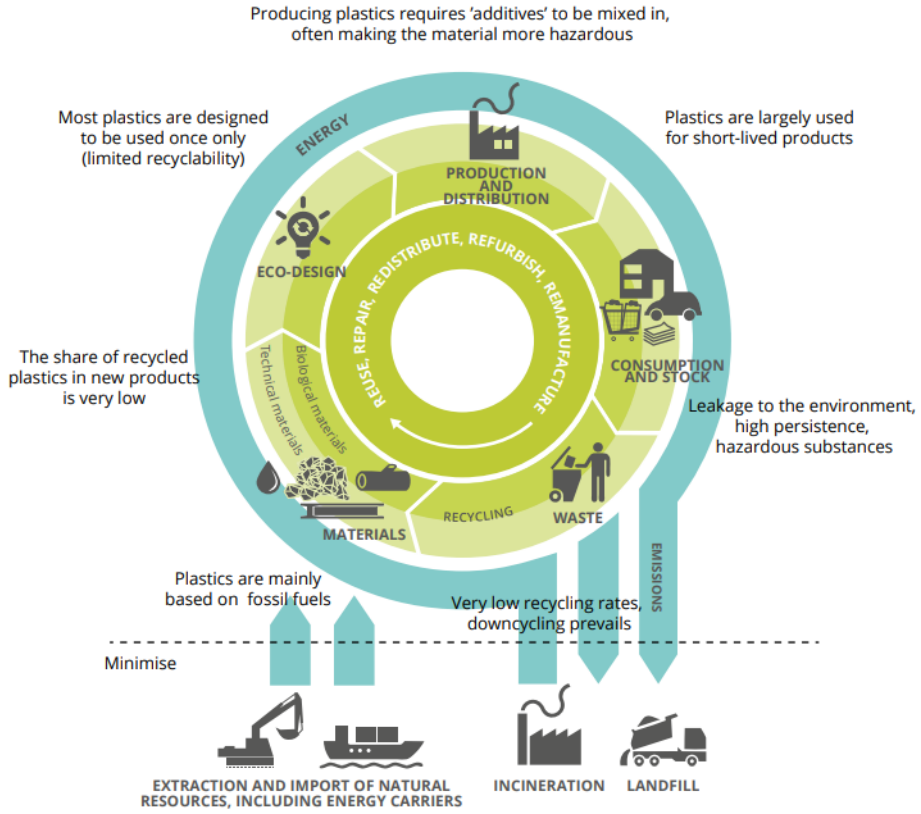

Figure 1. Overview of the environmental and systemic impacts of the global plastic economy (Source EEA 2021, information searched 12.11.2024).

Microplastics are plastic fragments which are 1 µm to 5 millimetres in diameter. Microplastics can result from the degradation of larger plastic products or from primary microplastics which are used as raw material in industry, as well as in beauty products and toothpastes (Ashrafy et al. 2023; NOAA 2024).

Microplastics have raised complex global issues because there are currently no natural organisms that can consume plastics as food (Bank et al. 2022). This means that plastics can only degrade into smaller pieces (microplastics and nanoplastics). The additives in plastics can also be of concern when they end up leaching into the environment, ingested by fish and other organisms (EEA 2021). In addition to the detrimental effects of plastic ingestion on organism health, microplastics can carry co-contaminants that may leach from the digestive system into other parts of the body (Bank et al. 2022). Co-contaminants that may enter the organism's body upon ingestion are substances such as flame retardants, lubricants, lead, copper, DDT, PAHs, PBTs. (Bank et al. 2022 s. 69).

Plastics are widely transported by the erosion forces of wind, water and gravity due to plastics often being lightweight (EEA 2021). However, as there is for example a water

cycle on Earth where water gets recycled repeatedly through the various spheres that exist on our planet, plastics don't get recycled the same way water does, as plastics only get degraded to smaller pieces (Bank et al. 2022; Carr et al. 2016). Since organisms cannot utilize plastics as food because they do not decay, plastics' end destination through erosion often ends up being oceans, landfills, lakes, and mountain ranges (Abel et al. 2023; Bank et al. 2022 s.7).

It is of particular importance to study estuarine and other waterfront areas, such as the Turku Archipelago Sea in terms of their microplastics abundance, as nearly all marine microplastics originate from terrestrial areas must first migrate through estuaries, rivers and other waterfront formations before dispersing more widely in oceans (Abel et al. 2024; Carr et al. 2016; Cole et al. 2011; Thompson et al. 2009; Van Cauwenberghe et al. 2015). Marine plastic litter consists 80% of plastics that are of terrestrial origin (Cole et al. 2011). López et al. 2021 study shows that estuaries with tributaries can function as "sinks" for microplastic accumulation, which is why it is important to examine how heavily these fresh and brackish water ecosystems are affected by microplastic pollution. What increases the abundance of plastics in these waterfront areas even further is that nearly half of the world's population lives within 80 km of a coast (Cole et al. 2011). Major sources of plastics and microplastics introduced into waterfront areas include cosmetic products, textiles, packaging materials, agriculture, and road infrastructure, including car tires (Carr et al. 2016; Cole et al. 2011; Thompson et al. 2009; Bank et al. 2022).

3. Materials and methods

3.1 Study site

The sediment core used in this study was taken from the bottom sediments in the middle of a semi-enclosed basin next to the island of Haverö, Finland, from a depth of around 20 metres. In this enclosed basin of Haverö, oxygen depletion prevails, causing there to be no bioturbation activity by living organisms which allows for better preservation for varved sediments (Jokinen et al. 2018; Zolitschka et al. 2014). The distances to the mouths of the largest rivers in the area, the Aurajoki River and the Paimionjoki River, are 25 km and 38 km, respectively (Jokinen et al. 2018). A small brook runs into the basin originating from a lake located on the Haverö island (Jokinen et al. 2018). The study area is surrounded by the smaller islands of Småholmen, Utterholm, Morsholmen, Mörholm,

Ramsholmen and Hässjeholmen, which may protect our study site from general wave action which allows fine sediments to settle down at the bottom more readily and resuspension being minimized (Zolitschka et al. 2014) (Figure 2). Glacio-isostatic rebound has resulted in progressively calmer depositional conditions in the area (Jokinen et al. 2018). Anthropogenic influence on the basin is minimal and population on the Haverö island is sparse. The dominant direct anthropogenic influence on the basin's nutrient loading came from two fishing cages that were operational from 1987 to 2008 CE (Jokinen et al. 2018).

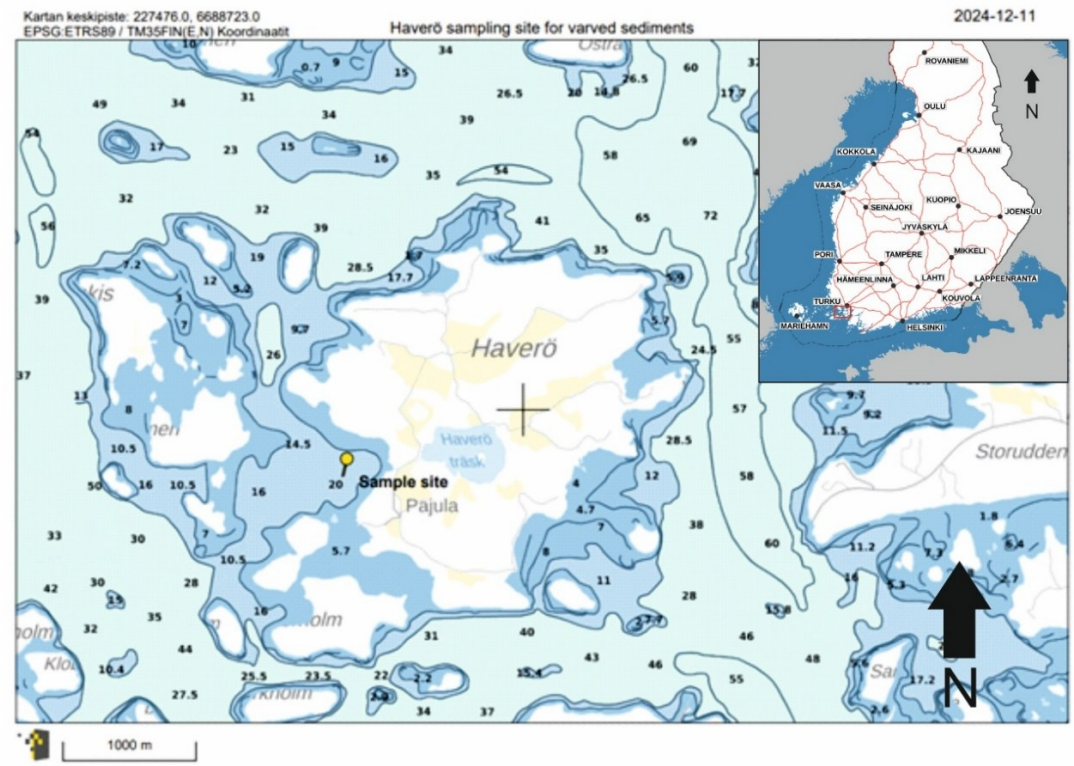

Figure 2. Haverö basin with the sample site marked with a yellow pin. Numbers on the map represent water depth (in meters). (Source: Paikkatietoikkuna.fi, information searched on 12.11.2024.

3.2 Sampling methods

The sediment core retrieval was done aboard the Aurelia research vessel owned by University of Turku on 31st of October 2024. The retrieval was done using an Uwitec-surface corer (Figure 3a) with additional weight of around 40 kg for the corer to ensure sufficient penetration into the sediments. The Uwitec-surface corer can be assembled and

stored in a metal box (Figure 3a). It consists of different metal rods, screws, acrylic sample tubes, rubber seals, and the customizable 10-kilogram metal weights. After lifting the Uwitec-corer sample from the sediment bottom, a smaller two-meter PVC sample tube was inserted into the collected sediment to obtain a slightly smaller diameter (7.4 cm) sample to facilitate the splitting of the sediment core. PVC tube was sealed with paper towels and plastic caps (Figure 3b & 3c).

Figure 3a. Uwitec surface-corer, 3b Sample tube which was sealed for transportation. 3c Smaller diameter sample tube inserted into the Uwitec surface-corer sample tube. The top of the sample tube was sealed with paper to prevent the sediment from leaking upon transportation (Photos taken by: Henri Heikkinen on 31. Oct 2024).

The collected sample was stored in the cold-storage room at 5°C for a duration of around two weeks until subsampling and measurements were taken. For subsampling, the PVC tube that stored the varved sediment sample had to be split in two halves from top to bottom horizontally with a circle saw. Precision was needed at this step for not to needlessly contaminate the sediment sample with PVC sawdust. Once the sample tube was cut in half, there existed two varved sediment sequences in tubes that were both used in the upcoming subsampling stages. The surface of the sediment sequence was cleaned with glass slips, and high-definition photos were taken of the whole sediment record before the LOI subsampling process (Figure 4).

Figure 4. A high-definition image taken of the entire split-core sample tube marked with pins every 10 varve years up from 2024 to ±1924 (Photo taken by: Henri Heikkinen on 4th of Dec 2024).

3.3 Magnetic susceptibility

According to Blumentritt & Lascu (2015), magnetic susceptibility (MS) is a common proxy for identifying clastic materials and soil erosion in sediment cores. MS measurements can be taken from multiple cores from the same water basin and correlated together. MS can also be used for cross-correlation and to assess the magnetic fraction of the sediment core. MS results can also aid in varve counting in addition to being non-destructive, inexpensive method that isn't time-intensive (Blumentritt & Lascu 2015). MS is a measure of the ability of a material to be magnetized in the presence of a small magnetic field (Thompson et al. 1975). MS measurements were taken with Bartington MS2 instrument which was set to scan the low field magnetic susceptibility of the varved sediment sample tube every 2 mm starting from the youngest varved sediments at the top and ending the scan 1 m deep into the sample tube. The sample tube was covered in a plastic film that was spread evenly throughout the whole sediment core to avoid the sensor from getting dirty when in contact with the sediment surface. The MS measurement was done as a split-core scan. In total, Bartington MS2 took 500 individual measurements. Low field susceptibility measurements were taken from the smaller diameter sediment core also used for the LOI measurement. Prior to taking the measurements, a calibration sample was used to calculate the potential drift. Additionally, an air reading was taken which was used to calculate the corrected MS value.

3.4 Water content and loss-on-ignition (LOI)

Water content of the sediment was measured based on the mass differences between freshly collected sediment and how much mass was lost when the sediment was dried overnight in a Memmert-oven at 105°C. The equation being fresh sediment weight subtracted from dried sediment weight (Figure 9).

With LOI (Loss-on-ignition) measurements it's possible to determine the organic matter and carbonate mineral content in sediments. It has been a standard procedure in

sedimentological studies for decades now since the implementation due to its accessibility (Sansisteban et al. 2004). The LOI method utilizes differential thermal analysis, where organic matter starts to combust around 200°C and is fully consumed by approximately 550°C. Carbonate minerals decompose at higher temperatures, with calcite breaking down between 800 and 850°C and dolomite between 700 and 750°C (Sansisteban et al. 2004).

After MS measurements, the measured half of the sediment core was systematically sampled into 60 different crucibles which represent 60 annual sediment accumulation cycles. First, each of the crucibles were weighed without a sample and all the weights were entered into an Excel spreadsheet. After this, one year's worth of varved sediment was scooped using a scalpel was scooped out of the PVC tube and carefully placed in the crucible. This means that the sample was destroyed in the process; however, the other half of the PVC tube, which was cut in half, was still stored in cold storage and was used for later measurements. The sample was then weighed in the crucible and marked alongside the number of the varved sediment year in question. This process was repeated for every 60 of the crucibles.

The next step was to dry out all of the water in the samples in the Memmert oven at 105°C and to obtain the dry weight of the sample which was then also weighed and documented. Next was the heating of the subsamples in 550°C (for four hours) to find out how much organic carbon is lost through combustion from the sample in elevated temperatures. This percentage difference in weight between the dried samples at 105°C and 550°C was then measured. This study also investigates the amount of carbonate material burned at 950°C. The same procedure was repeated as for the samples heated at 550°C, but at 950°C for two hours. After heating at both 550°C and 950°C, the samples were immediately placed in a desiccator to cool for approximately 15–20 minutes, to avoid moisture absorption that can occur while the samples are still hot. Since the mass losses during heating are exceedingly small, any moisture uptake could affect the reliability of the results.

The data gathered from LOI sampling was converted into an excel diagram by using the following mass loss percentage formulas commonly used in LOI calculations. The former one being used for the samples heated at 550°C and the latter used for the samples burned at 950°C (Heiri et al. 1999, Heiri et al. 2001, Sansisteban et al. 2004).

$$LOI_{550} = \left(\frac{DW_{105} - DW_{550}}{DW_{105}}\right) \times 100$$

Equation 1. Where LOI550 represents LOI at 550 °C (as a percentage), DW105 represents the dry weight of the sample before combustion and DW550 the dry weight of the sample after heating to 550 °C (both in g) (Heiri et al. 2001)

$$LOI_{950} = \left(\frac{DW_{550} - DW_{950}}{DW_{105}}\right) \times 100$$

Equation 2. In a second step, carbon dioxide is evolved from carbonate, leaving oxide and LOI is calculated as: where LOI950 is the LOI at 950 °C (as a percentage), DW550 is the dry weight of the sample after combustion of organic matter at 550 °C, DW950 represents the dry weight of the sample after heating to 950 °C, and DW105 is again the initial dry weight of the sample before the organic carbon combustion (all in g) (Heiri et al. 2001).

To calculate the amount of carbonate material present in the samples the following equation is used: 1.36 x LOI 950°C (Heiri et al. 2001, Sansisteban et al. 2004). Carbon dioxide weighs 44 g mol^{-1} and carbonate (CO_3^{2-}) weighs 60 g mol^{-1}, necessitating a conversion when calculating the carbonate content (Heiri et al. 2001).

3.5 Measuring varve thicknesses using ImageJ

The thicknesses of the varved sediments and individual laminae were measured digitally using imageJ line measurement tool from high-definition pictures taken of the sample sediment tube (Figure 9). This measurement was performed on 16 of the most recent varves, dated from 2009 to 2024. Graphs were made for the biogenic laminae, minerogenic laminae and total varve thicknesses.

3.6 Subsampling for microplastic analysis

After taking LOI measurements, the spare half of the sediment core covered by tin foil was taken out of cold storage, and the sediment was scooped out of the PVC tube one varve at a time. For this study, varved sediments that are up to 60 years old were analysed using 60 glass containers. First, the glass containers were washed with tap water, then with distilled water, and lastly with filtered (0.2 µm GFF glass fibre filter) Purelab UHQ water. This was done to avoid any airborne microplastics or microplastics already existing

in the containers. This process, hereafter referred to as rinsing, was repeated every time a new varved sediment sample was placed in the container. Rinsing also includes all instruments that are used in handling the sediment or that come into contact with the microplastic samples.

It was important to ensure that each varve year matched those used for the LOI samples from the other half of the sediment core. A photo reference of the sample tube was used to ensure that this process was successful alongside placing pins after every 10 varve years to minimize errors in counting.

The average weight of the five glass containers was 14.743 grams, and this average was used in the later calculations, as the weight differences between the glass containers weren't substantial. The varved sediments from the sediment core were individually scooped and placed into small, rinsed glass containers. The weights of the varved sediment samples were noted down in Excel upon sampling.

After the previous process, all 60 of the samples were stored overnight in a freezer. The next stage of subsampling was freeze-drying the samples in a vacuum with Christ Alpha 1-4LD plus freeze-drying machine. The samples were placed in the machine for 24 hours at -25°C and 0.63 mbar. Following this initial phase, a final drying phase took place for 4 hours at -50°C and 0.040 mbar. Upon completion of the freeze-drying process, all 60 samples were reduced to brittle dust, making them significantly lighter due to the removal of water.

A decision was made to use another sediment core sample from the same study site as the first core to increase the total sample size and to obtain more accurate readings of the microplastic particles that are in the Haverö basin. Earlier tests done using FTIR-imaging revealed that the microplastics particle amounts were too low using one sediment core.

Density separations were be done on 30 of the most recent varves. Previously taken photographs were used to match the varves with those subsampled from the sediment core used for LOI measurements. The varves were almost identical, and could be correlated visually, since both sample tubes were taken from approximately the same location. This new sample tube was larger in diameter (90 mm), and fresh sediment was used instead of freeze-dried material. Using two different sample tubes is more complex and time-consuming but may be necessary when there is insufficient sample material to obtain quantitatively reliable microplastic results.

The topmost 16 varves (2009–2024) were selected for enzyme purification stages and FTIR-imaging to save resources due to the time-consuming nature of sediment treatment. Freeze-dried samples were combined with the fresh sediment samples with matching varve chronology in the rinsed Teflon tubes and the density separation was done for each sample representing one year of sediment deposition.

3.7 Blank samples

When working with such small objects as microplastics, human errors are bound to happen. One way to account for errors and to assess the laboratory contamination is to use blank samples (Raynie 2018). Three blank samples were made, and they were treated as the real samples, and they underwent all the same filtering and enzymatic purification as is described in the following method sections in order to assess how much microplastic contamination the real samples experience.

3.8 Density separation

A single varve of fresh sediment was divided into two or three Teflon tubes, and the total weight of a single varve was tallied up. The weights of each freeze-dried sediment samples were calculated after measuring the weight of the fresh sediment sample and it was done by first measuring the weight of the Teflon tube and the fresh sediment sample, then pouring in the corresponding freeze-dried varved sediment sample and subtracting the weight difference that came from adding the freeze-dried sample. The weight of ten Teflon tubes was measured, and an averaged weight was used when calculating the weights of the varved sediment samples (36.069 g).

When all sediment that could be collected from the crucible and glass jar had been transferred to the Teflon tube, LST heavy liquid (density ~2.0 g/cm^3) was added until the tube was nearly full but still able to be shaken. The tube was then shaken by hand and using a Vortex Genie 2 shaker. When everything inside the tube was mixed, the tubes were placed inside of the VWR® Mega Star 1.6 General Purpose 1.6 L Benchtop Centrifuge. The samples were placed inside the centrifuge for 14 minutes at 3655 RPM. The centrifuging caused the potential microplastics particles to float to the surface of the LST heavy liquid and the minerogenic sediment to sink to the bottom of the tube. When using fresh aqueous sediment rich in clay minerals, the separation was not perfect but sufficient for this study and does not significantly affect later filtration steps. Scaly clay

particles are very light, and they can aggregate together with organic compounds, making it difficult to make them sink to the bottom using the centrifuge.

After the centrifuging process finished, the samples were carefully placed in the drawer cabinet to not stir up the sample. The LST heavy liquid and floating microplastic particles were carefully poured into the rinsed glass jar from the Teflon tubes minimizing the amount of sediment transferred into the glass jar. The inside walls of the Teflon tube were also carefully washed with UHQ water to get microplastic particles that might be stuck on the walls of the Teflon tube into the glass jar. The sediment often adhered to the bottom of the Teflon tubes, making this procedure possible; however, this was not always the case when the sediment was too loose. LST heavy liquid could then be added again to the Teflon tubes still containing the sediment and potential microplastic particles until the Teflon tube was almost full. This whole process was repeated twice with LST heavy liquid and once with UHQ water to ensure the high recovery of microplastics from the sample sediments.

Because of the availability of Teflon tubes and due to the centrifuge being able to handle only 16 samples tubes at one time, the remaining sediment could be discarded after the three rounds of LST heavy liquid separation and one round of UHQ water centrifuging. The Teflon tubes were then washed and cleaned thoroughly with water as was done in the previous stages and the process could be done for the next varved sediment samples.

3.9 Enzymatic processes overview

Löder et al. (2017) have discovered an effective method for purifying and filtering microplastics out of sediment samples using different types of enzyme treatments which break down organic matter, cellulose, proteins, and lipids etc. from the sediment samples, leaving behind only the untouched microplastic particles. Löder et al. (2017) call this stage of the microplastic research the Basic Enzymatic Purification Protocol (BEPP) of which a modified version of is used in this research (Figure 5). After this step was completed, the subsamples could be utilized FTIR-spectroscopy where the microplastic particles could be seen, counted, and analysed.

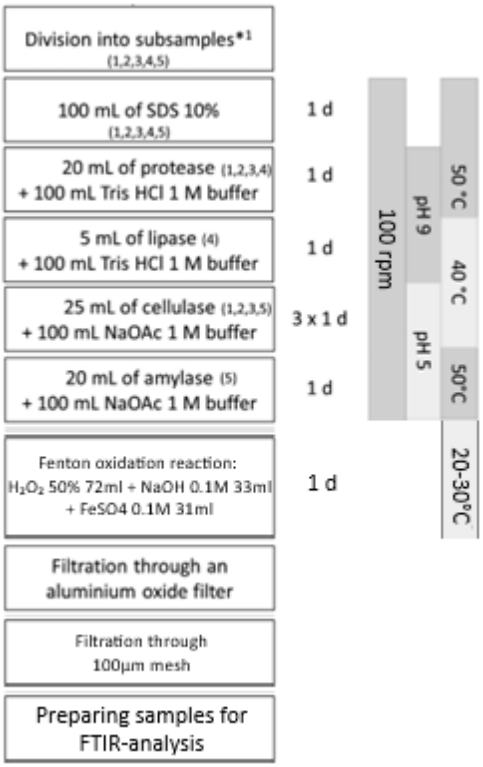

Figure 5. Löder et al. (2017) Universal enzymatic purification protocol modified version for the purposes of this research edited by: Henri Heikkinen.

3.9.1 Filtering out LST Heavy Liquid

LST Heavy Liquid was filtered out using aluminium filters with a mesh size of 15 µm and a diameter of 40 millimetres. A bottle-top filtration system with suction was used to filter and rinse out the used LST and later the buffer solutions which was also used in all the later stages of BEPP (Löder et al. 2017) (Figure 6). LST Heavy Liquid was poured through the aluminium oxide filter which was tightly sealed in place on the bottle-top filtration system to not lose microplastic particles. This left behind only the microplastics and organic/inorganic material that were too large to pass through the filter. The filter was then carefully lifted off the bottle-top filtration system and placed into a vial using thoroughly cleaned laboratory pliers.

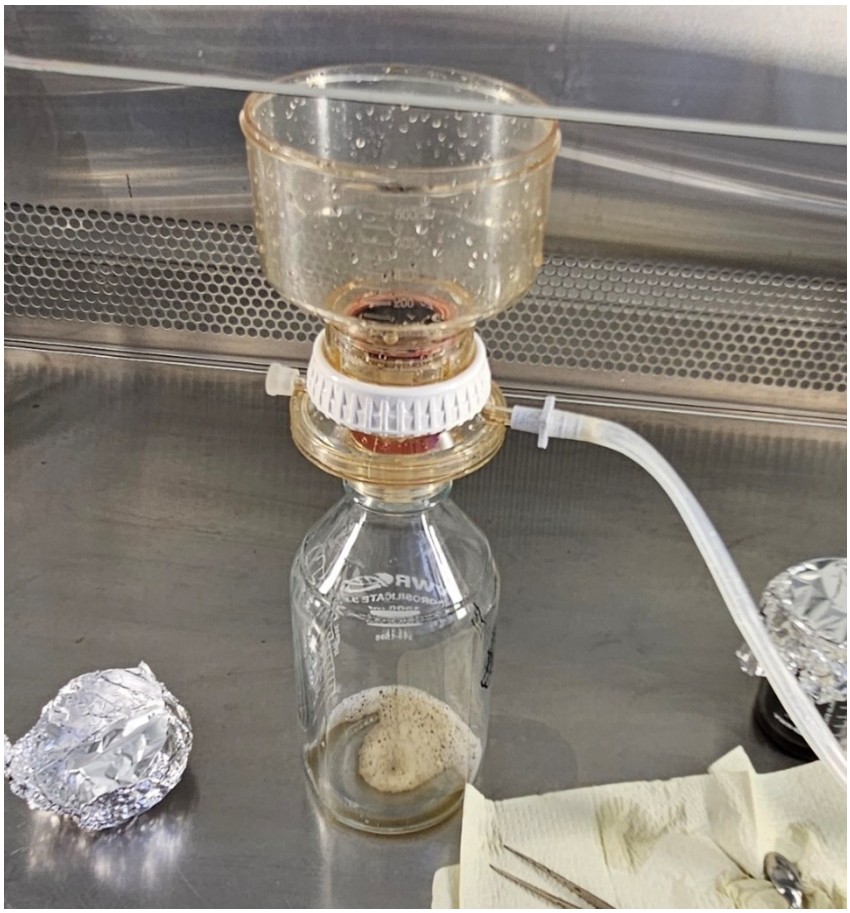

Figure 6. Bottle-top filtration system which is made from HDPE and was used throughout all microplastic purification stages (Picture taken by: Henri Heikkinen).

3.9.2 Sodium dodecyl sulphate treatment (SDS)

According to Löder et al. (2017), sodium dodecyl sulphate treatment is the first stage of the enzymatic treatment process. SDS acts as an anionic surfactant to soak out planktonic organisms and plant- and animal residues. The first step was to measure the right weight of SDS pellets and place them into water and stir the water until the pellets were in solution to create 10 % SDS solution. Before use, the SDS solution, as any other liquid used in contact with microplastic samples during the sample pretreatment, was filtered through 15 µm aluminium filters, to reduce possible microplastic contamination of the solution.

Because some of the organic/inorganic material that was poured through the aluminium filter also ended up on the bottle-top filtration system, the next step was to rinse the bottle-top filtration system and its parts into the vial the aluminium filter was placed in. 10% Sodium dodecyl sulphate (SDS) solution was taken into a syringe and with the precision

and pressure coming from the syringe, SDS was used to clean around and under the bottle-top filtration system and its parts to not lose microplastics particles. Precision was required in this step, as the syringe must be used while the bottle-top filtration system was held over the vial to ensure that the SDS and potential microplastics are deposited into the vial rather than on the laboratory table.

A total of 60 ml of SDS was added to the vial to cover the aluminium filter(s) (Löder et al. 2017). After this step, 16 vials containing the SDS solution, aluminium filters, microplastics and other debris left over from the density separation were placed into an incubation chamber (Infors HT Ecotron) for 24 hours that's running at 50°C and 100 RPM (Löder et al. 2017). It is important to note that every piece of the bottle-top filtration system and any tools that were used in all preparatory stages were washed thoroughly, first with tap water, then with distilled water and finally rinsed with UHQ water to minimize laboratory contamination and the cross effects of any of the detergents, buffer solutions and enzymes might have had with one another.

3.9.3 Protease treatment

In the protease treatment stage, a buffer solution of Tris hydrochloride (HCl) was used. The pH was titrated to a pH of 9 using HCl. The titration process was similar to the process of titrating SDS, and the solution was filtered using aluminium filter before use.

During the protease treatment, decomposition of protein chains into easily dissolved and dispersed peptides is catalysed by the protease enzyme (Löder et al. 2017). This stage of the enzymatic purification protocol follows laboratory procedures similar to those used in the LST heavy liquid filtration and SDS treatment stages. First, the SDS was filtered through a new aluminium filter that's held in place by the bottle-top filtration system (Figure 6). This left behind only the microplastics and other debris on the aluminium oxide filter. The filter was taken out with pliers and carefully placed at the bottom of the vial. After this a syringe was filled with a TRIS buffer solution and then the edges and bottom of the bottle-top filtration system were cleaned thoroughly to ensure that no potential microplastics were left on the filtration system. Once 100 ml of Tris HCl was in the vial, the protease enzyme (ASA Protease A-01 Spezialenzyme GmbH) was run through a fresh clean aluminium oxide filter to remove potential debris and microplastics and to minimize contamination. After this, 20 ml of protease enzyme was poured into the vial that contains the buffer solution and the aluminium oxide filter from our sample. The

vials were placed in the incubator (Infors HT Ecotron) for 24 hours at 50℃ and spinning at 100 RPM (Löder et al. 2017).

3.9.4 Lipase treatment

According to Löder et al. (2017), the lipase enzyme treatment stage was added to the BEPP after the protease treatment stage to account for lipids released during the digestion of food, biota, and water samples containing organic plant or algal material. This stage of the enzymatic treatment protocol largely followed the same procedures as in the protease treatment stage. The buffer solution used was still Tris HCl with the same pH 9. However, only 5 ml of lipase enzyme was poured into the vial containing the 100 ml of Tris HCl buffer solution. The temperature was also lowered to 40°C for the 24h incubation period but the RPM of 100 was kept the same.

3.9.5 Cellulase treatment

The cellulase treatment targets the maceration of phytoplankton cell walls and other plant residues and it is the third stage of the BEPP after SDS treatment (Löder et al. 2017). The buffer solution was changed to be NaOAc (Sodium acetate, CH_3COONa) at this stage of the treatment. The pH of the NaOAc buffer was ensured to have a pH of ~5 (AAT Bioquest, Inc. 2025). In order to get the desired pH, acetic acid (CH_3COOH) was poured into the solution until the pH reached ~5. Once the pellets were in solution with the water and the pH reached the desired value, more distilled water was added until the container was filled to the 1 litre mark.

The NaOAc solution was also filtered through an aluminium oxide filter to remove impurities. NaOH was prepared by first pouring 800 ml of distilled water into a glass container and weighing out (40 grams) of sodium acetate pellets for a 1 M buffer solution. The sodium hydroxide pellets were slowly added to the distilled water due to a common thermal reaction with the water.

When the NaOAc buffer solution was prepared for use, the cellulase treatment stage largely followed the same steps as in the preceding sections. It is important to mention that the syringe that's used in all the BEPP stages had to be thoroughly washed especially when the buffer solution was changed. This process was done by using tap water, distilled water and finally UHQ water.

Once there was 100 ml of NaOAc buffer solution in the vial with the sample, 25 ml of cellulase enzyme (ASA Cellulase TXL, Spezialenzyme GmbH) was poured in. The temperature in the incubation chamber was set to 40°C and RPM 100 for 24 hours (Löder et al. 2017). The difference between this treatment stage compared to the previous ones was that after the incubation period, the sample in the vial usually looks grimy and it might be hard to pour through the aluminium filter. If this was the case, NaOH was used to make the filtration easier. When enough NaOH (~50-100 ml) was added to the solution containing the sample, cellulase enzyme and NaOAc, the precipitates dissolve and the sample was significantly easier to pass through the filter.

3.9.6 Amylase treatment

The final enzyme purification stage in these samples was to use amylase enzyme (ASA Amylase, Spezialenzyme GmbH) after the cellulase treatment stage to further digest degradation products such as food, biota, organic plant, or algae content (Löder et al. 2017). The buffer solution was the same as in the cellulase treatment stage (NaOAc) and largely followed the same steps as was laid out in the preceding sections. Once filtered, 100 ml of NaOAc 1 M was added to the sample vial alongside 20 ml of filtered amylase enzyme. The sample vials were put into the incubation chamber at 40°C and RPM 100 for 24 hours. After the incubation period the samples were even more grimy than what they were post cellulase treatment. Around 100 ml of NaOH was poured in until the grime dissolved and the sample could be passed through the aluminium oxide filter.

3.9.7 Fenton oxidation reaction

After the SDS, protease, lipase, cellulase and amylase treatment stages, leftover debris persisted, including clay and mostly organic particles that remained in the samples alongside the microplastics. The goal was to eliminate as much of this debris as possible in order for FTIR-imaging to provide clearer data about the microplastics contained in the samples. The amylase enzyme was filtered through the aluminium filter as done previously. This time, ~50 ml of UHQ water was added to the sample vials.

The next step was to prepare the samples for a Fenton-reaction. The aluminium oxide filters were completely removed from the samples by rinsing them thoroughly with pre-filtered UHQ water with enough pressure to ensure that no microplastics were left on the filters. Total amount of UHQ water now in the samples was between 75-120 ml.

30 grams of (Supelco) Iron (II) sulphate heptahydrate was measured using a measuring beaker. 1 litre of water was then added and the iron sulphate heptahydrate was mixed until it had all dissolved. The solution was moved to a glass beaker, where 12 ml of concentrated sulphuric acid was added to the solution. Additionally, hydrogen peroxide (H_2O_2) 50% was the other compound used in the Fenton-reaction. Both the iron sulphate solution ($FeSO_4$ + H_2SO_4) and hydrogen peroxide 50% had to be filtered through aluminium oxide filters to reduce the risk of contamination.

In preparation for the Fenton-reaction itself, multiple trays of ice cubes were put in the freezer overnight. The goal during the Fenton-reaction was to have the temperature in the beakers remain between 20 and 30°C for the reaction and it was achieved by placing the beakers into a tub full of cold water and ice cubes if the reaction temperature draws closer to 30°C. This was because there was risk for the microplastics contained in the beakers to melt or disintegrate if the temperature was to exceed 30°C. Thermometers were placed into the beakers to accurately monitor the temperature. To catalyse the Fenton-reaction, 72 ml of filtered 50% H_2O_2 was added to the beakers that already contained the samples and between 75 to 120 ml of UHQ water. The H_2O_2 already burned some of the organic compounds left in the samples. After this, 33 ml of 0.1M NaOH and 31 ml of 0.1M FeSO4 solution were added to catalyse the reaction.

In this study, the Fenton-reaction was comparatively mild, and lasting for around 5 hours, gradually weakening towards the end. There was a total of 19 samples in 19 different beakers. None of the samples reached critical temperatures where microplastics could have been disintegrated. The beakers didn’t overflow which could have caused a loss of microplastic particles. There was still some debris left over from the oxidation reaction such as PVC particles from the sample tube, clay, and silt particles but all organic compounds were eliminated.

3.9.8 Preparing the samples for FTIR-imaging

To prepare the samples for FTIR, the reagents involved in the Fenton oxidation reaction had to be filtered out using the bottle-top filtration system utilizing an aluminium oxide filter similar to previous stages of purification (Figure 6). Since the Fenton reaction eliminated all organic compounds from the samples, it was important to avoid the development of new mold or other organisms, which was why the aluminium oxide filter was rinsed into the test tubes using filtered 70% ethanol. The test tubes used here could

hold 50 ml of liquid and were thoroughly cleaned, along with a glass funnel used for rinsing the aluminium oxide filters. The glass funnel was placed inside of the test tube, and the aluminium oxide filters could be rinsed on top of it and finally the funnel itself was rinsed into the test tube. A total of 19 test tubes were needed for all the samples (16 for actual microplastic samples and 3 for system blank samples).

3.10 FTIR-imaging

FTIR-imaging was conducted in collaboration with University of Eastern Finland in Kuopio SIB laboratory using Agilent Cary 670 spectrometer and Cary 620 microscope. Fourier Transform Infrared (FTIR) Spectroscopy is used to determine the chemical composition of different particles (Uurasjärvi, 2021). In this study, the composition of various microplastic particles alongside the amount and diameters of different microplastics separated from the sediment samples was identified with FTIR-imaging.

It was determined that the microplastic sample tubes still contained too much residue from chitin, clay etc. which would have negatively impacted the results obtained from the FTIR-imaging. Thus, one last filtration was done to get more accurate results even if a portion of the smaller diameter microplastics had to be sacrificed. The filtration was carried out using a bottle-top filtration system similar to that used in the University of Turku microplastic laboratory, except that this one was made of glass. 50 µm mesh was first used on sample number 13, and 10 ml of the sample was poured through the filter, but the mesh size proved to be too small to get rid of all the chitin. An asterisk marks HH Hav 13, as 10 ml of sample material was poured directly onto the silver membrane (Table 1). For the remaining 27.5 ml amount of sample number 13 and the rest of the samples (excluding the three blank samples), a 100 µm mesh was used to get rid of the leftover residue. Notes were taken on the volume (in millilitres) of 70% alcohol in each sample tube before filtration, the amount of UHQ water used to rinse the filters into a measuring flask, and the amount of this UHQ water that was passed through the 5 µm silver-coated membrane used for FTIR imaging.

Three blank samples were first imaged using FTIR. Following preparations were done for all of the samples before the imaging could be conducted. The blank sample was poured through a 5 µm silver membrane with a 12 mm imaging area where all the particles would be concentrated in using the bottle-top filtration system. The bottle-top filtration system was rinsed with UHQ-water thoroughly to flush all the potential microplastics

onto the silver membrane. Afterwards, the silver membrane was glued onto a microscope glass slide, which was then placed inside a Petri dish to avoid contamination. The sample number and the volume (in mm) of sample that was poured through the silver membrane were marked on the Petri dish.

Many PVC particles remained in the sediment samples after the sample tubes were cut in half and have persisted throughout the subsequent processing steps, including all filtration procedures (excluding blank samples). It was decided not to pass all the sample material through the silver membrane to avoid excessive interference from larger PVC particles during FTIR imaging.

The measuring flask containing the sample was first stirred and then allowed to stand so that the larger PVC particles settled before the sample was slowly poured through the silver membrane, stopping before the larger PVC particles reached the membrane. The aim was to leave ~5 to 10 ml of UHQ water in the measuring flask after pouring. The remainder of the samples were collected into small glass bottles in case they are needed in the future. The amount of sample left in the measuring flask and how much was poured through the silver membrane was noted down (Table 1).

The blank samples were not filtered through a 100 µm mesh prior to FTIR imaging, as was done for the actual samples. This resulted in the blank samples containing smaller microplastic particles than the actual samples. In the process of filtrating the actual samples through the 100 µm mesh, microplastic particles under 100 µm were potentially lost. However, this filtration was necessary for the FTIR-imaging to take place. To mitigate this error in blank samples compared to the actual samples, microplastic particles whose major dimension didn’t exceed 100 µm were excluded from the table that was saved from siMPle as they would have most likely passed through the filter (Table 1).

Table 1. Notes on amounts of sample material used for FTIR-imaging

Sample number	Original sample (ml)	UHQ water in flask (ml)	Amount of UHQ water poured through 100 µm filter (ml)	Amount of sample leftover (ml)	Amount of sample poured without filtering (ml)	Amount of sample used total (%)	Amount Sample left (%)
HH Hav 1	40	50	45	5		90	10
HH Hav 2	40	46	40	6		87	13
HH Hav 3	40	50	45	5		90	10
HH Hav 4	40	45	40	5		89	11
HH Hav 5	37	40	35	5		88	13
HH Hav 6	40	45	40	5		89	11
HH Hav 7	38	50	40	10		80	20
HH Hav 8	42	50	40	10		80	20
HH Hav 9	40	50	43	7		86	14
HH Hav 10	41	50	42	8		84	16
HH Hav 11	41	45	40	5		89	11
HH Hav 12	40	56	46	10		82	18
HH Hav 13*	38	80	43	37	10	79	21
HH Hav 14	38	70	65	5		93	7
HH Hav 15	40	50	45	5		90	10
HH Hav 16	40	50	45	5		90	10

3.10.1 Analysis of FTIR-data and statistical methods

The FTIR imaging datasets were transferred to the siMPle software developed by Primpke et al. (2020) to obtain data relevant to microplastic research. The datasets were first converted to .hdr format, which is required by siMPle. Raw data .dmd files were then converted to .spe, after which the datasets could be analysed for spectra fit following loading the reference spectra library (.txt) in siMPle. The reference spectra library contains the spectra information for the most common types of microplastics, fibres, proteins, wool, and lipids (Primpke et al. 2020; Sainio 2023).

With siMPle, data concerning polymer type, MP size (height, width, number of pixels, mass, volume) and location on map were obtained for each sample individually. For every sample, a spreadsheet and a spectra map was then saved (Figure 7). Additionally, the spectra map shows particles such as proteins and cellulose which are excluded from the microplastic spreadsheets (Figure 7).

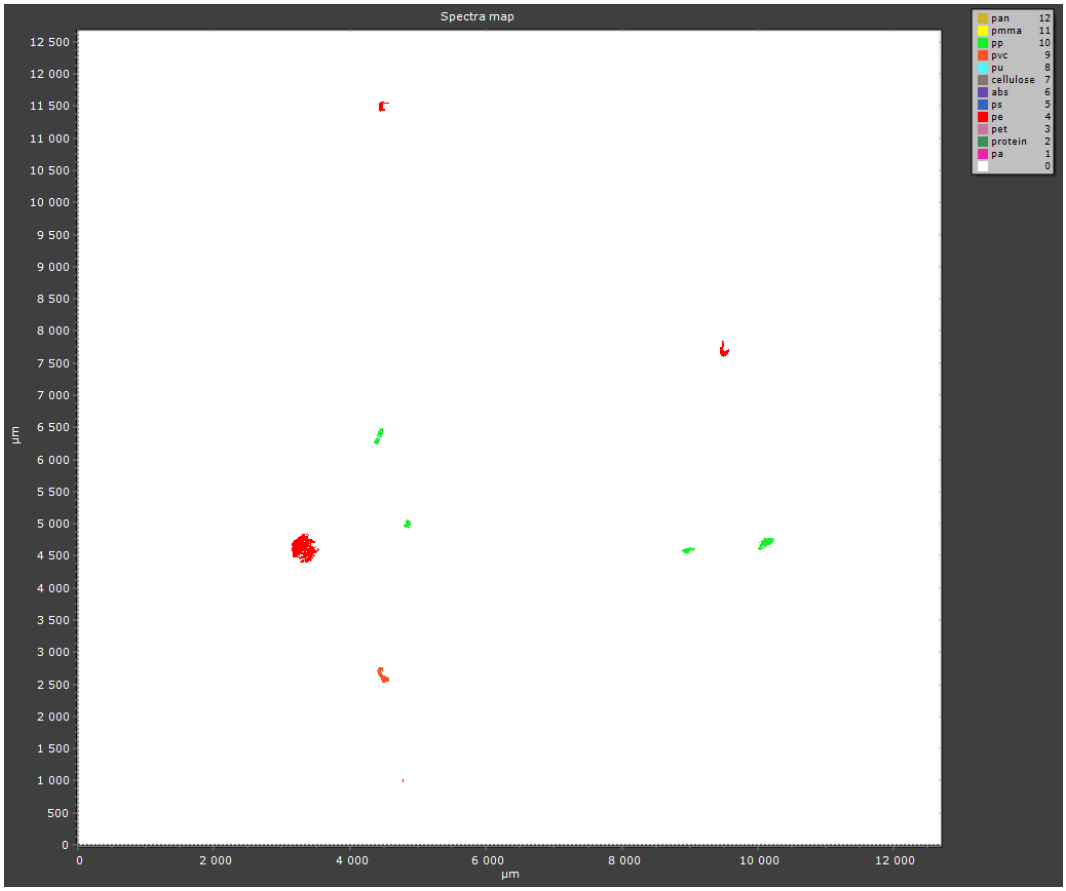

Figure 7. Spectra map of sample number 7. (2018) from siMPle-program displaying identified microplastic particles and their polymer types (red = polyethylene, green = polypropylene.

A concentration value was calculated based on the amount of dry sample used for each sample, by determining the average number of microplastic particles per gram of dry weight based on particles identified using siMPle. As an example for sample number 7, 13.976 grams of dried sample was used and 8 microplastic particles were identified with a concentration of 0.572 MPs/g. Concentration was used as a unit of measurement due to each varve not being uniform in thickness which means the data wouldn't be comparable between varve years. From the microplastic spreadsheets saved from siMPle, PVC particles were removed and not considered in the calculations since they mostly came from the saw dust when the sediment cores were cut open and PVC was not found in the blank samples either.

3.11 Accounting for laboratory contamination

Throughout the multiple stages of preparation and subsampling of sediment obtained from the bottom of the Haverö Basin, there are various points at which potential microplastic contamination may occur. This is to be expected in microplastic research especially from microplastics that are obtained from sediments. Human error should be minimized through proper guidance. Most of the subsampling was done in Geohouse's microplastic laboratory. To minimize microplastic contamination, all instruments and equipment used in every stage of subsampling, filtering and enzyme treatment stages were first rinsed with tap water, then with distilled water and finally with UHQ water. UHQ water was contained in a Teflon bottle, and the subsampling jars were made of glass. The surfaces of the fume hood were wiped with filtered 100% ethanol before and after use and all glass containers as well as decanters were covered with aluminium foil when not in use. Only 100% cotton lab coats and non-polyester clothing were allowed to be worn in the microplastic laboratory alongside nitrile gloves.

Despite all the cautionary steps, a noticeable amount of microplastic contamination was still unavoidable. A source of contamination was microplastic particles present in the microplastic laboratory, which can become airborne even in weak air currents and may settle in the samples. The bottle-top filtration system that was used in every filtration was made of hard plastic (HDPE) that may release small plastic fragments into the sample (Figure 6). Microplastics that are on the surface of skin, hair and clothing can fall into the samples if preventative measures, such as covering the samples with tinfoil, are not taken. Pre-washed polypropylene sample tubes in which all the samples were transferred to

University of Eastern Finland for FTIR-analysis could have also been a source of PP contamination.

In addition to microplastic contamination, a certain percentage of microplastic particles are bound to be lost during each stage of the subsampling, potentially the contaminant microplastics themselves. A major challenge of microplastic research is that the degree of contamination is truly visible only right at the very end of the treatment after the FTIR-datasets are obtained. However, the siMPle results indicate that the samples contained substantial amounts of MPs even after the samples were filtered through the 100 µm mesh. The blank samples also supported this, as microplastics with a major dimension under 100 µm were removed from the dataset, indicating that contamination was relatively minimal (Table 2)

The water content, organic matter and carbonate data for varve number two (2023) was also accidentally lost, resulting in a small gap in data (Figure 9).

4. Results

4.1 Low field magnetic susceptibility measurements

The MS values show that starting from the uppermost parts of the sediment core (the youngest sediments starting from 0 mm), the values alternate largely between 10 and 35 and slightly trend towards 35 when moving downward in the sediment core. However, around the 450 mm mark where there is a sudden peak in MS which reaches a peak value of 52, highest in the sediment core (Figure 8). According to varve calculations, this peak occurred around 1994. After the peak, there's a small drop in susceptibility at the 474 mm mark that goes down to 20.5. After this drop, a steady alternating pattern continues with values ranging from 20 and 30 until the end of the segment of the sediment core that's used in this research between 474-580 mm. The peaks in MS values are not as drastic or rhythmic after 474 mm as the MS values in the earlier parts of the sediment core (Figure 8).

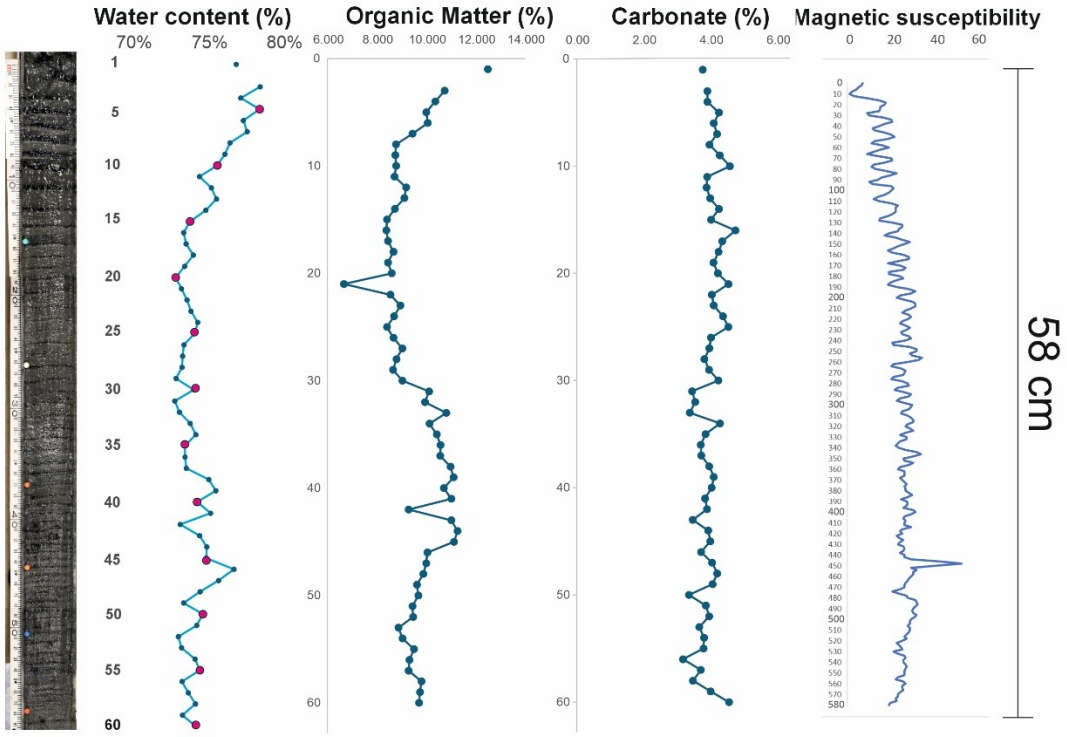

Figure 8. From left to right; fresh sediment sample where pins marking every 10th varve year, water content (%), Organic matter (%), Carbonate material (%), and Magnetic susceptibility (MS).

4.2 Water content and LOI

The measured water content in the sediment ranges between ~80-73% (Figure 8). Higher values in the uppermost parts of the sediment tube with the more recent varves, gradually decreasing to a water content range of 74% at varve number 16. The water content doesn't rise over 78% for the remainder of the graph and a peak value of 78% is found at varve number 46 (Figure 8).

Organic matter and carbonate amounts vary in the samples (Figure 8). The minimum value for organic matter is found at varve number 21 (6.66%) and the maximum value at varve number one (12.5%). For carbonate material the minimum value occurs at varve number 50 (3.35%) and maximum value at varve number 16 (4.73%) (Figure 8). Organic matter in the sediment follows a pattern similar to water content. The upper part of the sediment (the topmost seven varves) contains higher organic matter, which decreases with depth. The content then remains relatively constant until around varve 30, after which it increases slightly again (Figure 8). After varve number 45 the organic matter content drops again to a similar range that's found in the upper parts of the core. Carbonate

material in the core hovers consistently between 3-5% with no remarkable peaks in either direction except for three observable low years between the varves 31-33 (1993-1991) (Figure 8).

4.3 Varve thickness

The thickest minerogenic lamina in this review section of the sediment core was formed during 2015 and was 15.42 mm in diameter (Figure 9). The second thickest was from 2017 where the minerogenic lamina measures 15 mm in diameter (Figure 9). The calculated average for minerogenic lamina was 11.5 mm (Figure 9).

The biogenic laminae become progressively thinner when going downwards in the sediment core, showing the top 5 thickest biogenic laminae in topmost 0-8 cm (Figure 9). The calculated average for biogenic lamina thickness was 2.77 mm (Figure 9). The total varve thickness follows the trends in minerogenic lamina thickness, with calculated average for total varve thickness being 14.2 mm (Figure 9).

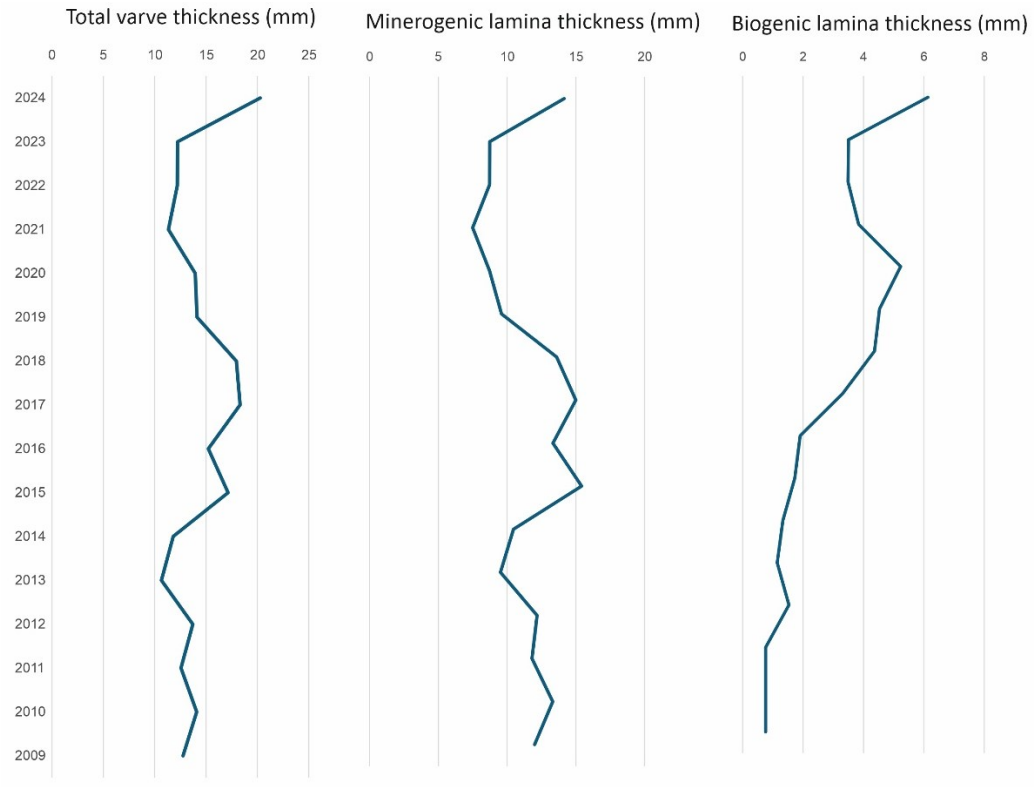

Figure 9. Annual changes in varve composition from 2024 to 2009, displaying the thickness (in mm) of total, minerogenic, and biogenic laminae.

4.4 Microplastic data from FTIR and siMPle

High-resolution datasets from FTIR-imaging were compiled of each sample. Mosaic images and FTIR spectra analysis reveal that not every piece visible was a microplastic on the silver membrane that was imaged (Figure 10).

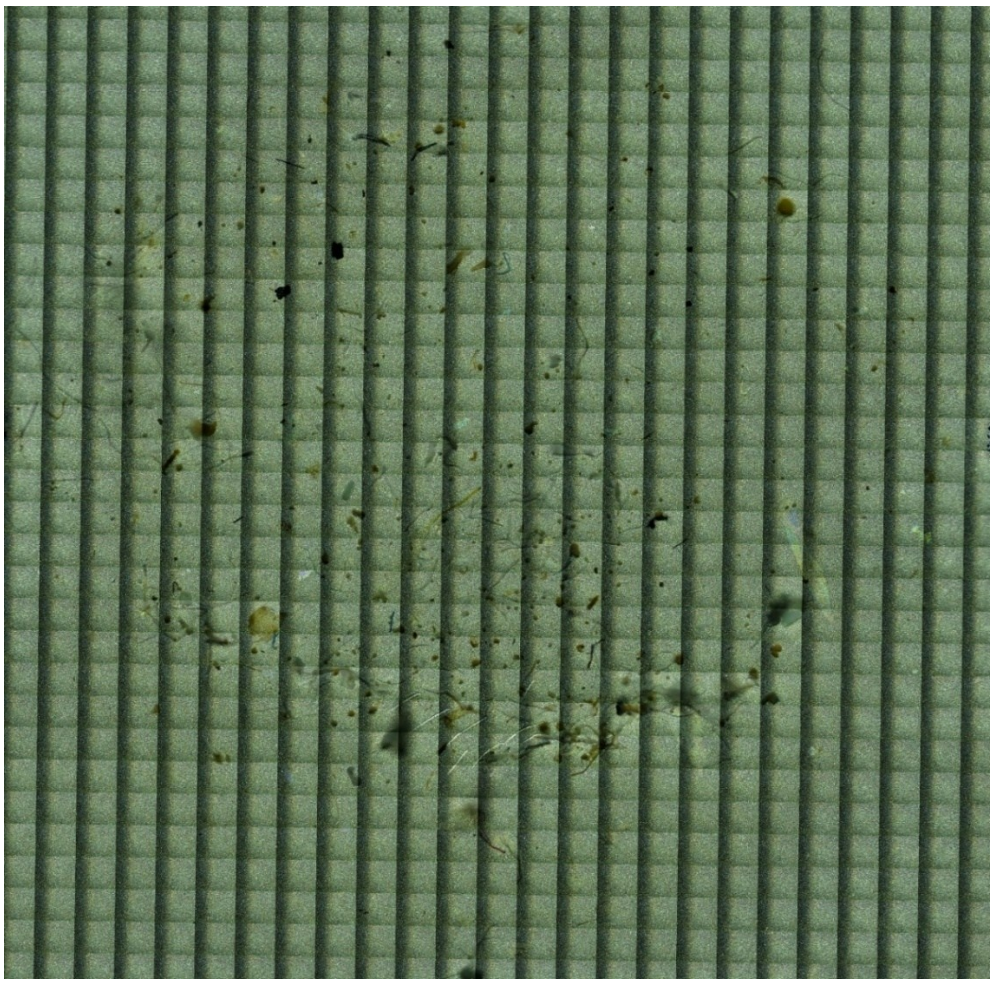

Figure 10. Screenshot taken of Sample number 7. (2018) from FTIR-software after scanning a mosaic image of the sample. All fragments visible aren't necessarily microplastics (Photo taken by: Henri Heikkinen).

The samples are dominated mostly by polyethylene (PE) and polypropylene (PP). Low number of polystyrene (PS) were also found alongside one polyamide (PA) microplastic particle (Figure 11). The distribution of polymer types across the full dataset of 16 samples is as follows: from the 258 MP particles found, 129 of them were PE (50%), 112 PP (44%), 16 PS (6%) and 1 was PA (0.004%) (Figure 11).

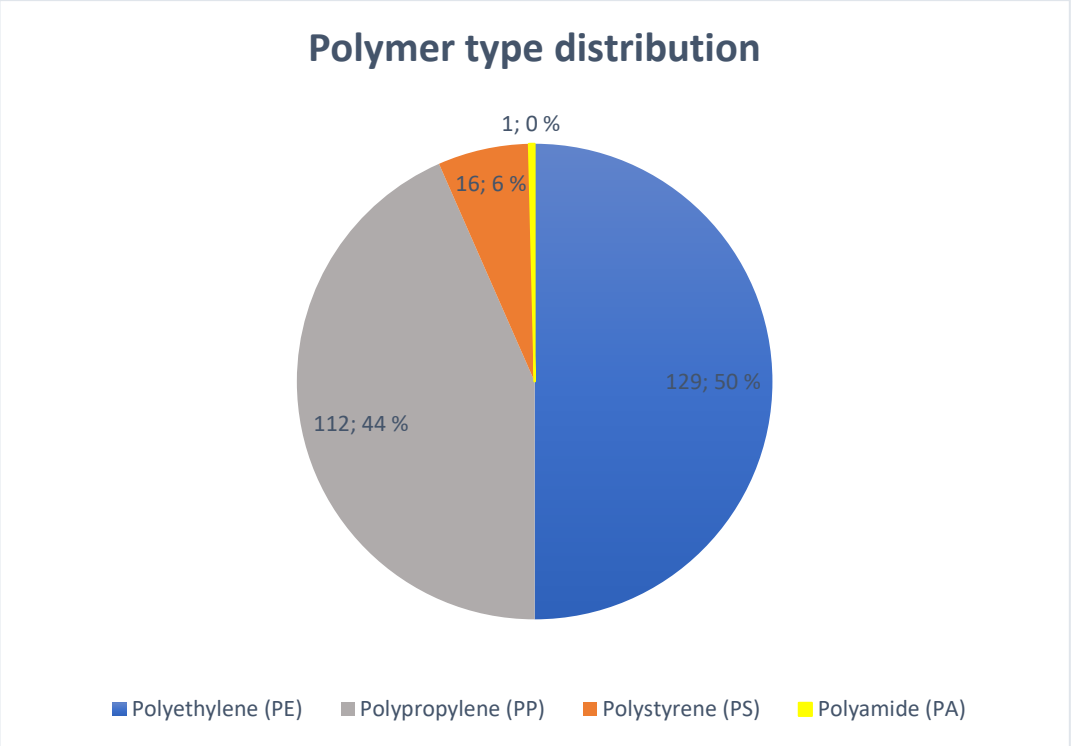

Figure 11. Polymer type distributions across all 258 MPs found in the 16 sediment samples that were analysed using FTIR.

Microplastic concentrations are consistently higher starting from 2020 upwards, with sample number 5 (2020) having a concentration value of 2.327 MPs/g (the highest out of every sample) (Figure 12). The second highest concentration was found in sample number 4 (2021) with a concentration of 1.941 MPs/g. Polystyrene (PS) was found in larger amounts in the upper varves as compared to the lower varves. PE was the dominant polymer type in most samples and was found in every sample (Figure 12).

A total of 258 microplastic particles were identified from a total of 256.65 grams of DW sediment across all 16 samples. The concentration of microplastics across the whole observational period of 16 varve years equates to 1.005 MPs/g of dry sediment. Given

that virtually all microplastics under 100 µm were lost during filtration, the actual concentration was likely higher.

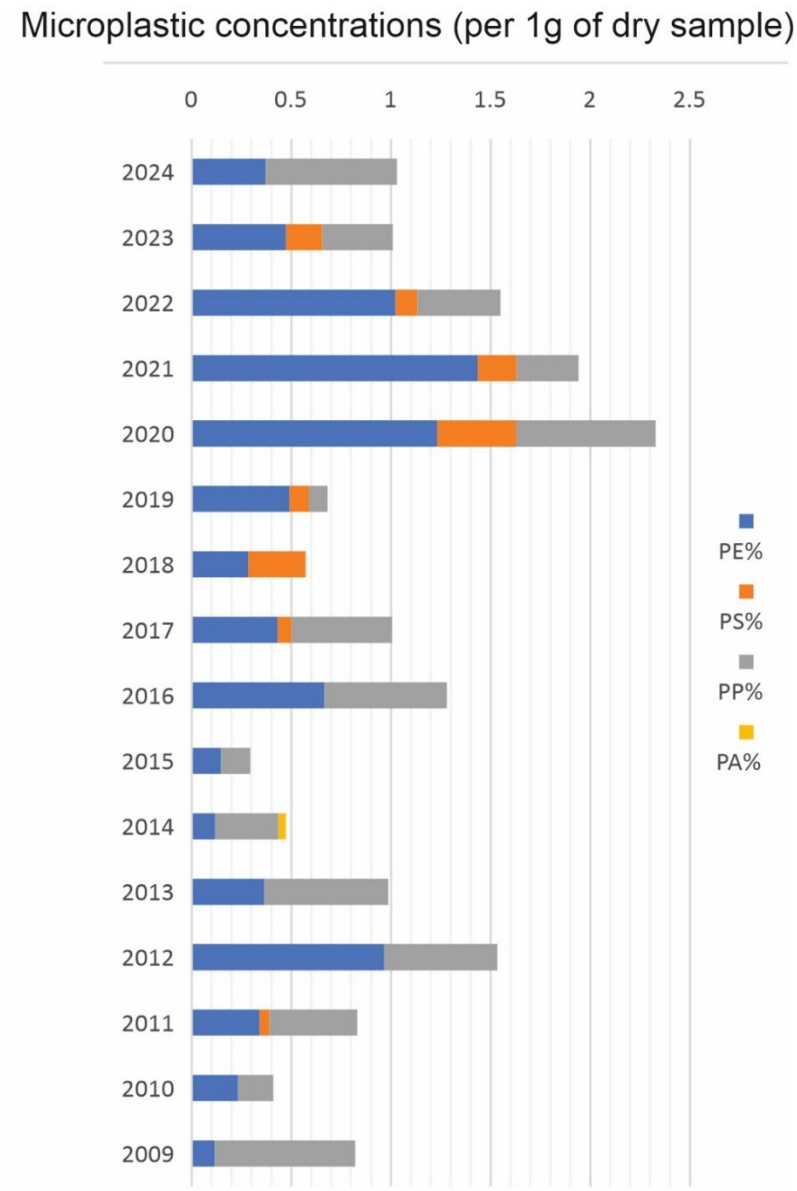

Figure 12. Annual microplastic concentrations (MPs/g) between the years 2024-2009 by polymer type PE= polyethylene (blue), PS= polystyrene (orange), PP= polypropylene (grey), and PA= polyamide (yellow). Each coloured sequence of a bar expresses the percentage of how much of a single polymer type was present in each sample.

The majority of the particles appear to have jagged edges and are irregularly shaped (Figure 13). Some PP microplastic particles appear to have an elongated or fibrous shape. Some PE particles appear to be slightly more rounded than other particles which might indicate the particle being a microplastic bead regularly used in cosmetic products. Most

PS particles also appear to be bead-shaped. The singular PA particle identified in sample number 11 was fibrous in shape (Figure 13).

Figure 13. Demonstration of typical microplastic particles for each polymer type identified with siMPle.

4.5 Microplastics in blank samples

Microplastics found in blank samples are as follows: size fraction >100 µm HH blank 1 had 9 MPs, HH blank 2 had 9 MPs and HH blank 3 had 3 MPs. Blank samples between the size fractions of 10 µm to 100 µm showed MPs in the following quantities: HH blank 1 27 MPs, HH blank 2 59 MPs, HH blank 3 18 MPs (Table 2).

Table 2. All MPs found in the blank samples

HH blank 1	Polymer group	Major dimension [µm]	Minor dimension [µm]	Mass [ng]
MP_4	pe	130.6	29.5	33.9
MP_6	pe	128.9	74.1	211.3
MP_7	pe	149	38	64.2
MP_8	pe	224.6	27.6	51.0
MP_9	pe	140.2	30.8	39.6
MP_10	pe	105.5	23.4	17.1
MP_20	pp	447.8	160.5	3442.2
MP_24	pp	106.2	47.5	71.5
MP_25	pp	110.8	47.3	73.8
9 MPs				
HH blank 2	**Polymer group**	**Major dimension [µm]**	**Minor dimension [µm]**	**Mass [ng]**
MP_4	pe	578.3	136.7	3223.7
MP_5	pe	137.8	31	39.5
MP_20	pe	99.2	45	60.0
MP_36	pe	139.9	57.3	136.8
MP_37	pe	765.1	132.5	4008.7
MP_41	pe	145.3	59.1	151.5
MP_53	pp	155.6	41.8	81.2
MP_55	pp	98	38.9	44.2
MP_56	pp	119.1	41.7	61.8
9 MPs				
HH blank 3	**Polymer group**	**Major dimension [µm]**	**Minor dimension [µm]**	**Mass [ng]**
MP_2	pa	130.4	96.6	435.6
MP_9	pe	261	51.2	204.2
MP_12	pp	104.4	69.4	149.8
MP_13	pp	175.2	26.6	36.9
4 MPs				

5. Discussion

5.1 Sediment characteristics

The Haverö basin is relatively isolated and is enclosed by the small surrounding land masses and islands (Jokinen et al. 2018) (Figure 2). There are regular ferry/boat routes running next to the island of Haverö, but they do not directly cross the study area. This could have an influence on the microplastics that are carried to the bottom of the Haverö basin. There isn't a notable amount of anthropogenic activity in the near proximity of the Haverö basin except for small-scale fishing activity (Jokinen et al. 2018). Wave action currently has a greater effect on sediments in the Haverö Basin than it did around 1000 CE, due to reduced ice cover associated with global warming and ongoing glacio-isostatic uplift (Jokinen et al. 2018). This suggests that sediment in the Haverö basin is more concentrated in the middle of the basin due to wave action, resulting into more sediment accumulation especially during stormy periods (Jokinen et al. 2018).

The water content in the sediment gradually decreases when moving downwards into the older sediment structures (Figure 8). This is mostly explained by compressional forces that the upper sediments exert on the lower sediments through gravity, which cause the sediment to be more condensed and water to be squeezed out (Haltia-Hovi et al. 2007; Maier et al. 2013). The biogenic laminae are thicker closer to the top in the sediment core (Figure 9). The biogenic laminae contain less minerogenic content than the grey minerogenic laminae, which is why the biogenic laminae are more susceptible to compaction than the more minerogenic grey laminae (Haltia-Hovi et al. 2007; Maier et al. 2013). Water content and organic matter graphs are also markedly similar, which does makes sense considering that more organic matter was present in the biogenic laminae sections which tend to be more saturated with water thus easier to compact compared to the minerogenic laminae (Figure 9). There exists a section in the sediment core between the varves 30 and 45 which is more biogenic, which is also reflected in its water content and organic matter (Figure 8). It is noteworthy that in the topmost biogenic laminae, the organic matter has yet to begin decomposing to the same degree as what tends to happen to older sediment structures (Meyers & Ishiwatari, 1993), which explains the higher OM % and thicker biogenic laminae at the topmost sediments.

Haverö basin sediments receive a steady influx of carbonate material which has stayed consistent during the years of 1964-2024 (Figure 8). This influx of carbonate material has

likely resulted from plankton or the shells of clams which break down in waves and get crushed on beaches after which resuspension carries the fragments to the Haverö basin. This is supported by the chitin shells that remained in the samples even after Fenton-reaction and was observed under a microscope before filtering the samples through the 100 µm mesh.

5.2 Varve characteristics

The formation of varves in marine areas depend largely on environmental and sedimentological conditions (Schimmelmann et al. 2016). The area needs to have high sedimentation rates and the bottom needs to be oxygen-depleted, as it negates potential bioturbation activity. Seasonally fluctuating sedimentary input also helps to verify a noticeable varve pattern in the sediment (Jokinen et al. 2018; Schimmelmann et al. 2016, Zolitschka et al. 2015).

Many of the principles of varve formation, which Zolitschka et al. describe in their 2015 publication on varved sediments in lacustrine environments, also apply to marine settings, with certain exceptions concerning the more enclosed nature of lakes compared to marine systems. Variations in varve thicknesses can occur due to rainfall fluctuations between different years where more clastic material is eroded and it travels longer distances through streams and rivers (Zolitschka et al. 2016, Schimmelmann et al. 2016). Minerogenic content in marine sediments, in contrast to lake sediments, is strongly influenced by storm-triggered water level changes and the resuspension of sediments (Jokinen et al. 2015). Same applies for biogenic material which may be transported to the sedimentation site but may also be formed autochthonously, close to the sedimentation site (Zolitschka et al. 2015). During longer and warmer growth seasons, more biogenic material can form, and thus the biogenic lamina for that year is thicker, given that the biogenic material is preserved and does not degrade over time (Jokinen et al. 2018).The sediment core used in this study presents a clear visual example of such alternating patterns that can be found in typical varved sediments (Figure 4).

A trend of increasing MS value is found when moving downwards in the core (Figure 8). The cause of this increase can be explained by the diamagnetism of water and the water content being lower further down in the core leading to higher MS values (Gutiérrez-Mejía & Ruiz-Suárez, 2012). MS graph also has a clearer alternating pattern in the upper parts of the core and less so but still identifiable in the lower parts of the core. This could

be explained by the stronger contrast between the water rich fresh biogenic laminae at the surface, with decomposed organic matter and decreased water content within biogenic laminae towards the deeper sediments (Meyers & Ishiwatari, 1993). Nearly all varves were laid out relatively horizontally and only a few of the varves observed in the sample tube were crooked, suggesting that sedimentation occurred evenly. There was clear cleavage between each varve year when subsampling the sediment. (Figure 9). The total varve thickness peaks around 2024 (20.5 mm) for the sampling range between the years of 2009-2024 and the overall thickness of the varves remains relatively constant (Figure 9). The total varve thickness and minerogenic laminae thickness graphs appear similar, mainly because the minerogenic laminae are generally thicker than the biogenic laminae in the sample tube. This causes the mean values to resemble the minerogenic laminae trend (Figure 9). A decreasing trend in biogenic laminae thickness is observed during the earliest 16 varve years. A subsequent increase in biogenic laminae thickness is noted somewhere between varve years 30 to 45, a pattern that is also reflected in the water content data (Figure 8 & Figure 9). The biogenic laminae between the varves 30 to 45 are not as thick as in the topmost biogenic laminae but this is partly explained by the degradation which affects the older biogenic laminae in addition to possible compaction which affects the varve thicknesses (Maier et al. 2013; Meyers & Ishiwatari, 1993). It should be noted that the biogenic laminae are still thicker than the surrounding biogenic laminae between the varves 30-45 (1994-1979), possibly due to autochthonous production being higher between these years. The total thickness of the varves stay above 10 mm per year which indicates that the Haverö basin experiences reliable influxes of clastic and biogenic material every year which makes it an excellent site for varved sediment research (Figure 9) (Jokinen et al. 2015; Jokinen et al. 2018).

5.3 Microplastic characteristics

Individual varve thickness plays a role in how many microplastic particles may be found in each varve and how much sediment can be used for every varve that was analysed for microplastics. Since the amount of sediment and dried sample used for this study was relatively small, large-scale conclusions can’t be made concerning the actual polymer type distributions in the sample site. However, the results indicate that microplastics are present in every sample in varying quantities. The study of microplastics in varved sediment structures is still in its early stages which means that all data successfully collected is still valuable even if the sample sizes aren’t the largest (Martin et al. 2022).

With enough studies, certain patterns can emerge, even with smaller quantities of sample material that's processed.

A noticeable peak in microplastic concentration is found between the years 2020 and 2024 (Figure 14). The cause of this peak could be attributed to storms which leads to enhanced bottom water currents and lateral sediment transport (Jokinen et al. 2018) potentially including microplastics. However, the varves from 2020 to 2024 are only in between the ranges of 10-20 mm in thickness and the thickest varves in this dataset, 2018 to 2014 which range between 15-20 mm in thickness (Figure 14). This indicates that there is not necessarily a clear correlation between varve thickness and microplastic concentrations (Langknecht et al. 2024). Microplastic concentrations appear to fluctuate in cycles year by year (Figure 14). When comparing microplastic concentrations to total varve thickness, a pattern emerges suggesting a weak negative correlation; however, this relationship is not consistent across all varve years (Figure 14), making it an interesting observation (Figure 14). The cause of this negative correlation could possibly be explained by increased sediment flow during one year into the Haverö basin delaying the deposition of microplastics in the form of resuspension and during a calmer depositional year more microplastics can settle in the bottom and not get resuspended. Another possible hypothesis could be that increased sediment flow on more stormy years introduces higher load or coarser grain sized minerogenic particles to the basin which could "dilute" the microplastic concentration in the samples as there would be more minerogenic content than on calmer years even though net microplastic particle amount during a varve year might be higher than on some calmer years. This effect has also been noted in previous sediment trap research (Saarni et al. 2023). The former hypothesis is further supported the study done by Jokinen et al. 2018 on the Haverö basin where the gradual basin infilling resulted in more wave-induced sediment focusing to the deepest parts of the basin which enables coarser-grained sediments to accumulate during stormy years.

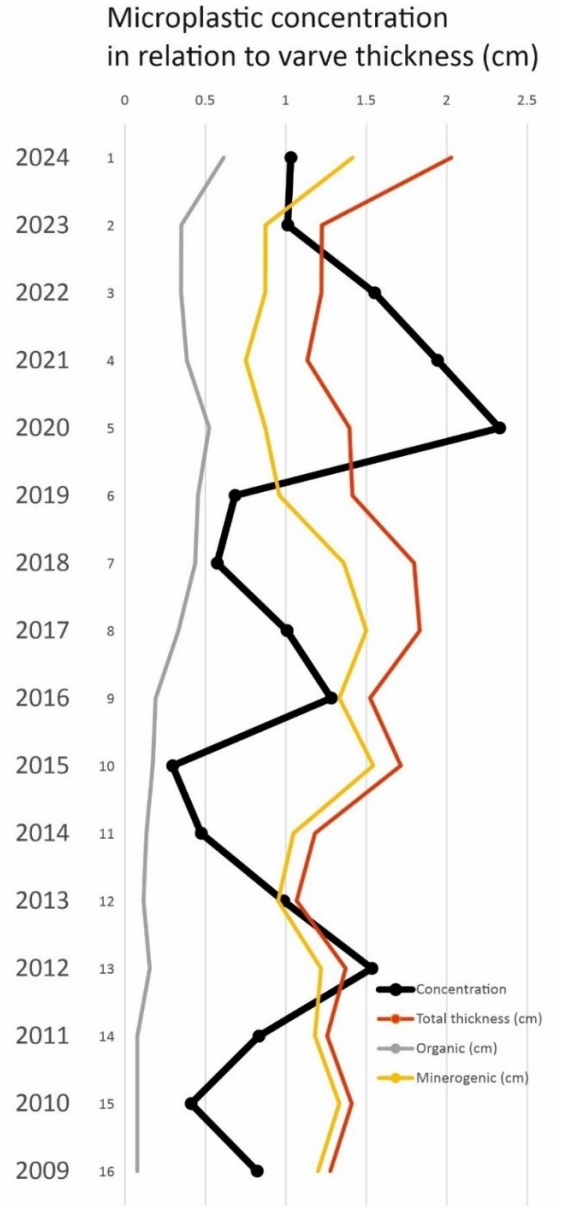

Figure 14. Microplastic concentration (MPs/g) in relation to varve thickness (cm). X-axis depicts both microplastic concentration value and the thickness of a single varve in centimetres. Y-axis depicts the varve year from (2024 to 2009) and sample number.

Explaining the presence, quantities, and concentrations of microplastics in the sediment involves a complex interplay of multiple variables, including natural processes, anthropogenic influences, and local geography. Consequently, it is difficult to identify the dominant sources of microplastics in the Haverö Basin (Jokinen et al. 2018; Langknecht et al. 2024; Martin et al. 2022). Based on the 2018 study done by Jokinen et al. on the Haverö basin, a potential source for microplastics in the basin could be from the small brook of Haverö island that runs into the basin and could potentially source microplastics from the island. The island of Haverö also houses a fish farm that uses plastic nets and

buoys which may contribute to the microplastic load of the basin (Jokinen et al. 2018). Other major sources of microplastics could originate from boats and ships that pass through the Haverö basin which could cause indirect microplastic loading in the form of plastic-based paint chipping or direct microplastic loading coming from littering. Aeolian deposition likely also plays a role in the amounts of microplastics that get transported into the Haverö basin and this includes surface currents such as waves (Cole et al. 2011; EEA 2021, Meyers & Ishiwatari, 1993). Varved sediments prove to be an excellent data source for microplastic research (Zolitschka et al. 2015; Cole et al. 2011). It is observed from the data that PS increased in abundance starting from 2017 moving towards the present day (Figure 12). Microplastic contamination and microplastic particles lost during the processing of the samples must also be considered when interpreting the data. Another observed caveat was that, during the final filtration step prior to FTIR imaging, the samples were saturated with chitin remains from small organisms that had settled in the Haverö Basin.

Spectra map of HH blank 2 (Figure 15) which contained significant amounts of MPs suggests that a larger PE MP particle got in the blank sample at a certain point in time and got broken down into tinier MPs throughout the process of filtering and subsequent treatment stages.

The microplastic polymer type distributions found in the samples reflect those that are typically found in sediments (Meronen 2020; Karim 2021; Langknecht et al. 2024; Lehto 2023; Sainio 2023). PE being the most abundant, followed by PP and PS. In larger volumes of sample material PA and PET could also be found in larger quantities (Langknecht et al. 2024). PE, PP & PS are also the most produced and used plastic types globally, which explains the plastic distributions also found in this research (Geyer et al. 2017).

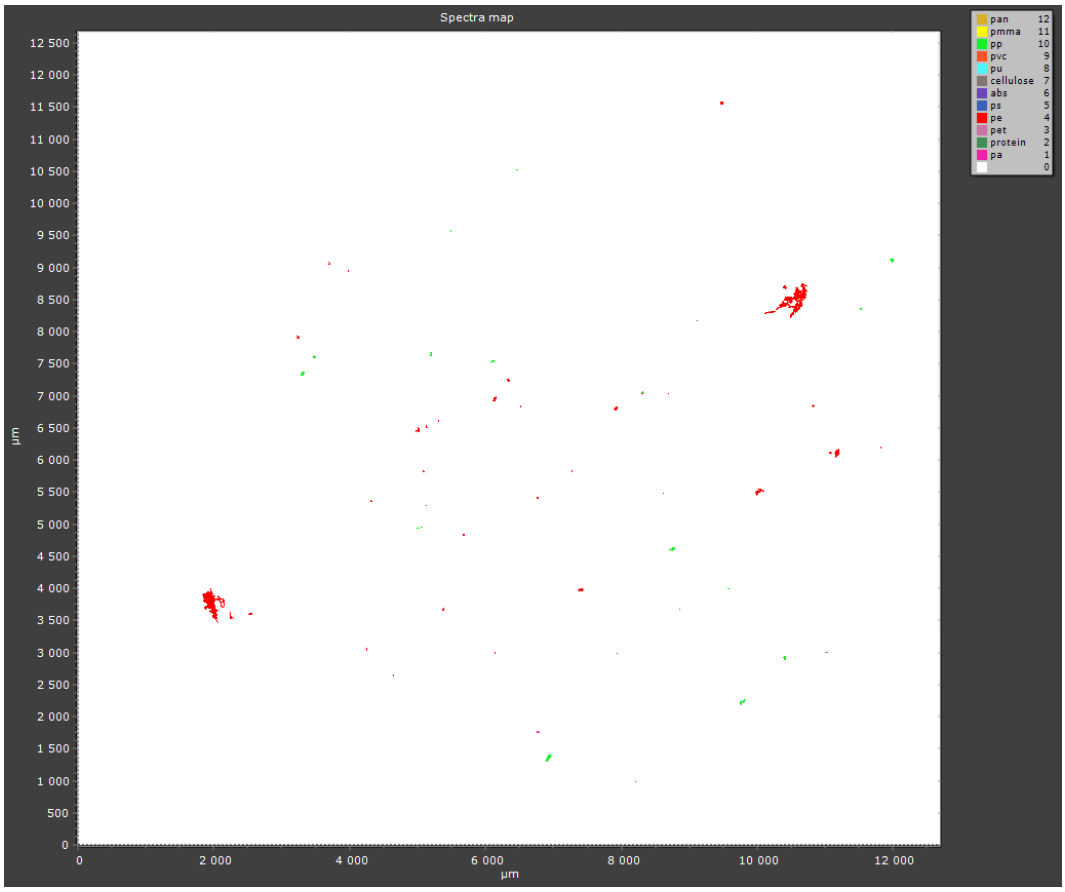

Figure 15. Spectra map of HH blank 2 saved from siMPle-program showcasing identified microplastic particles and their polymer types (red=polyethylene (PE), green= polypropylene (PP), violet= polyethylene terephthalate (PET).

6. Conclusions

Microplastic abundance, polymer type and concentrations were investigated in Haverö enclosed hypoxic basin located in Turku Archipelago Sea from varved sediment samples using a novel approach to microplastic research. Varved sediments can provide a much-needed temporal perspective into microplastic accumulation throughout the ever-increasing plastic ecosystem in which we live. The methodologies used to obtain microplastic data from varved sediment samples were time-intensive; therefore, only the past 16 years of data were used for microplastic analysis, despite the availability of additional varved sediment records. Water content, organic matter, MS and varve thickness data suggest that the sediment has undergone a noticeable degree of compaction in the lower parts of the sediment core. Magnetic susceptibility data reflects the presence of annually laminated sediment structures, displaying clear alternation between the biogenic and minerogenic laminae. Following the enzymatic purification protocol, the plastic polymers were identified using Fourier Transform Infrared (FTIR) Spectroscopy (Figure 5) and siMPle software. A total of 258 microplastic particles were found from 256.65 g of sediment (dry weight). Observed microplastic concentrations in the Haverö basin from 16 varved sediment samples spanning the years 2009 to 2024 were found to be 1.006 MPs/g. Microplastic amounts, and consequently concentrations, were likely reduced because all samples had to be filtered through a 100-micrometer mesh prior to FTIR imaging. This was necessary since the samples contained large quantities of chitin shells, which could have interfered with the quality of the FTIR data. For future research, chitinase enzyme treatment is encouraged. PE was the most abundant polymer type found in every sample. PP was also found in nearly every sample, and the ratios of each polymer type align well with findings of previous microplastic research. The main finding from this study is that this novel approach for investigating microplastics in annually laminated sediments is feasible and enables temporal insights into microplastic abundance and polymer types between individual varve years. This research can be used as a framework for future research on microplastics and for implementing further optimizations for the methodologies used in this research.

Acknowledgements

First and foremost, I would like to give thanks to my thesis supervisor Saija Saarni for guiding me through countless hours of laboratory work steps required in the sample preparation stage and overseeing my thesis writing. A big thanks also goes to the crew aboard the University of Turku research vessel Aurelia and Tuomo Soininen for guiding my work with FTIR and siMPle while visiting University of Eastern Finland. Lastly, I would like to give thanks to the people working at University of Turku and Geohouse.

References

Abel, S.M. *et al.* (2023) 'Journey to the deep: plastic pollution in the hadal of deep-sea trenches.', *Environmental Pollution*, 333, p. 122078. Available at: https://doi.org/10.1016/j.envpol.2023.122078.

Ashrafy, A. *et al.* (2023) 'Microplastics Pollution: A Brief Review of Its Source and Abundance in Different Aquatic Ecosystems', *Journal of Hazardous Materials Advances*, 9, p. 100215. Available at: https://doi.org/10.1016/j.hazadv.2022.100215.

Bank, M.S. (ed.) (2022) *Microplastic in the Environment: Pattern and Process*. Cham: Springer International Publishing (Environmental Contamination Remediation and Management). Available at: https://doi.org/10.1007/978-3-030-78627-4.

Blumentritt, D.J. and Lascu, I. (2015) 'A comparison of magnetic susceptibility measurement techniques and ferrimagnetic component analysis from recent sediments in Lake Pepin (USA)', *Geological Society, London, Special Publications*, 414(1), pp. 197–207. Available at: https://doi.org/10.1144/SP414.6.

Carr, S.A., Liu, J. and Tesoro, A.G. (2016) 'Transport and fate of microplastic particles in wastewater treatment plants', *Water Research*, 91, pp. 174–182. Available at: https://doi.org/10.1016/j.watres.2016.01.002.

Chalmin, P. (2019) 'The history of plastics: from the Capitol to the Tarpeian Rock'. Available at: https://journals.openedition.org/factsreports/5071

Cole, M. *et al.* (2011) 'Microplastics as contaminants in the marine environment: A review', *Marine Pollution Bulletin*, 62(12), pp. 2588–2597. Available at: https://doi.org/10.1016/j.marpolbul.2011.09.025.

European Environment Agency (ed.) (2021) *Plastics, the circular economy and Europe's environment: a priority for action*. Luxembourg: Publications Office of the European Union (EEA report, no 2020, 18). Available at: https://doi.org/10.2800/5847.

European Environment Agency (ed.) (2024) *Plastics* (2024). Available at: https://www.eea.europa.eu/en/topics/in-depth/plastics (Accessed: 16 February 2025).

Geyer, R., Jambeck, J.R. and Law, K.L. (2017) 'Production, use, and fate of all plastics ever made', *Science Advances*, 3(7), p. e1700782. Available at: https://doi.org/10.1126/sciadv.1700782.

Gutiérrez-Mejía, F. and Ruiz-Suárez, J.C. (2012) 'AC magnetic susceptibility at medium frequencies suggests a paramagnetic behavior of pure water', *Journal of Magnetism and Magnetic Materials*, 324(6), pp. 1129–1132. Available at: https://doi.org/10.1016/j.jmmm.2011.10.035.

Heiri, O., Lotter, A.F. and Lemcke, G. (2001) 'Loss on ignition as a method for estimating organic and carbonate content in sediments: reproducibility and comparability of results', *Journal of Paleolimnology*, 25(1), pp. 101–110. Available at: https://doi.org/10.1023/A:1008119611481.

History of plastics • Plastics Europe (2021) *Plastics Europe*. Available at: https://plasticseurope.org/plastics-explained/history-of-plastics/ (Accessed: 16 February 2025).

Jokinen, S.A. *et al.* (2015) 'Varve microfabric record of seasonal sedimentation and bottom flow-modulated mud deposition in the coastal northern Baltic Sea', *Marine Geology*, 366, pp. 79–96. Available at: https://doi.org/10.1016/j.margeo.2015.05.003.

Jokinen, S.A. *et al.* (2018) 'A 1500-year multiproxy record of coastal hypoxia from the northern Baltic Sea indicates unprecedented deoxygenation over the 20th century', *Biogeosciences*, 15(13), pp. 3975–4001. Available at: https://doi.org/10.5194/bg-15-3975-2018.

Kallenbach, E.M.F. *et al.* (2022) 'Microplastics in Terrestrial and Freshwater Environments', in M.S. Bank (ed.) *Microplastic in the Environment: Pattern and Process*. Cham: Springer International Publishing (Environmental Contamination Remediation and Management), pp. 87–130. Available at: https://doi.org/10.1007/978-3-030-78627-4_4.

Karim, S. (2021) 'Seasonal Variation of Microplastic Accumulation in Lake Sediments'. Available at: http://urn.fi/urn:nbn:fi:uef-20211105.

Langknecht, T. *et al.* (2024) 'The distribution of sediment microplastics assemblages is driven by location and hydrodynamics, not sediment characteristics, in the Gulf of Maine, USA', *Marine Pollution Bulletin*, 202, p. 116393. Available at: https://doi.org/10.1016/j.marpolbul.2024.116393.

Lehto, E. (2023) 'Mikromuovien esiintyminen Itämeren sedimenteissä ajan suhteen'. Available at: https://www.utupub.fi/handle/10024/176333 (Accessed: 9 December 2024).

Löder, M.G.J. *et al.* (2017) 'Enzymatic Purification of Microplastics in Environmental Samples', *Environmental Science & Technology*, 51(24), pp. 14283–14292. Available at: https://doi.org/10.1021/acs.est.7b03055.

López, A.G. *et al.* (2021) 'Estuaries as Filters for Riverine Microplastics: Simulations in a Large, Coastal-Plain Estuary', *Frontiers in Marine Science*, 8, p. 715924. Available at: https://doi.org/10.3389/fmars.2021.715924.

Maier, D.B. *et al.* (2013) 'Compaction of recent varved lake sediments', *GFF*, 135(3–4), pp. 231–236. Available at: https://doi.org/10.1080/11035897.2013.788551.

Martin, J., Lusher, A.L. and Nixon, F.C. (2022) 'A review of the use of microplastics in reconstructing dated sedimentary archives', *Science of The Total Environment*, 806, p. 150818. Available at: https://doi.org/10.1016/j.scitotenv.2021.150818.

Meronen, S. (2020) 'A density separation method for microplastics implemented to varved sediments of Lake Kallavesi, eastern Finland'. Available at: https://urn.fi/URN:NBN:fi-fe2020110689531

Meyers, P.A. and Ishiwatari, R. (1993) 'The Early Diagenesis of Organic Matter in Lacustrine Sediments', in M.H. Engel and S.A. Macko (eds) *Organic Geochemistry*. Boston, MA: Springer US (Topics in Geobiology), pp. 185–209. Available at: https://doi.org/10.1007/978-1-4615-2890-6_8.

Plastic Overshoot Day 2024: Global Waste Crisis Surpasses Management Capacity (2024) *SAFE - Safe Food Advocacy Europe*. Available at: https://www.safefoodadvocacy.eu/plastic-overshoot-day-2024-global-waste-crisis-surpasses-management-capacity/ (Accessed: 16 February 2025).

Primpke, S., Godejohann, M. and Gerdts, G. (2020) 'Rapid Identification and Quantification of Microplastics in the Environment by Quantum Cascade Laser-Based Hyperspectral Infrared Chemical Imaging', *Environmental Science & Technology*, 54(24), pp. 15893–15903. Available at: https://doi.org/10.1021/acs.est.0c05722.

Raynie, D.E. (2026) *The Vital Role of Blanks in Sample Preparation | LCGC International*. Available at: https://www.chromatographyonline.com/view/vital-role-blanks-sample-preparation-0 (Accessed: 4 April 2026).

Saarni, S. *et al.* (2023) 'Seasonal variation observed in microplastic deposition rates in boreal lake sediments', *Journal of Soils and Sediments*, 23(4), pp. 1960–1970. Available at: https://doi.org/10.1007/s11368-023-03465-3.

Santisteban, J.I. *et al.* (2004) 'Loss on ignition: a qualitative or quantitative method for organic matter and carbonate mineral content in sediments?', *Journal of Paleolimnology*, 32(3), pp. 287–299. Available at: https://doi.org/10.1023/B:JOPL.0000042999.30131.5b.

Schimmelmann, A. *et al.* (2016) 'Varves in marine sediments: A review', *Earth-Science Reviews*, 159, pp. 215–246. Available at: https://doi.org/10.1016/j.earscirev.2016.04.009.

Thompson, R. *et al.* (1975) 'Magnetic susceptibility of lake sediments', *Limnology and Oceanography*, 20(5), pp. 687–698. Available at: https://doi.org/10.4319/lo.1975.20.5.0687.

NOAA, US Department of Commerce, N.O. and A.A. (2024) *What are microplastics?* Available at: https://oceanservice.noaa.gov/facts/microplastics.html (Accessed: 16 February 2025).

Van Cauwenberghe, L. *et al.* (2015) 'Microplastics in sediments: A review of techniques, occurrence and effects', *Marine Environmental Research*, 111, pp. 5–17. Available at: https://doi.org/10.1016/j.marenvres.2015.06.007.

Zolitschka, B. *et al.* (2015) 'Varves in lake sediments – a review', *Quaternary Science Reviews*, 117, pp. 1–41. Available at: https://doi.org/10.1016/j.quascirev.2015.03.019.

Appendix 1

Microplastics identified with siMPle in sample number 1 (2024)), DW sediment:10.66 g, Amount of sample material used for FTIR: 90%.

HH Hav 1	Polymer group	Major dimension [µm]	Minor dimension [µm]	Mass [ng]
MP_1	pe	232.7	55.3	212.2
MP_2	pe	144	89.3	342.9
MP_3	pe	379.5	96.2	1048.4
MP_4	pe	210.9	62.7	247.0
MP_6	pp	239.7	49	171.8
MP_7	pp	30.1	15.4	2.1
MP_8	pp	221.8	133.2	1174.3
MP_9	pp	226	29.1	57.3
MP_10	pp	397.8	48.1	274.9
MP_11	pp	350.3	58.6	359.1
MP_12	pp	149.1	68.4	208.5

Appendix 2

Microplastics identified with siMPle in sample number 2 (2023), DW sediment:16.79 g, Amount of sample material used for FTIR: 87%.

HH Hav 2	Polymer group	Major dimension [µm]	Minor dimension [µm]	Mass [ng]
MP_1	pe	299.2	101.4	918.9
MP_2	pe	463.1	134.6	2502.9
MP_3	pe	177.4	74.2	291.9
MP_4	pe	217.6	34.3	76.6
MP_5	pe	72.2	30.9	20.6
MP_6	pe	157.3	62.4	183.0
MP_7	pe	454.2	153.5	3193.6
MP_8	pe	302.1	40.3	146.3
MP_9	ps	61.2	16.4	5.4
MP_10	ps	77.8	31.7	25.5
MP_11	ps	58.7	36.1	25.0
MP_12	pp	295.2	140.5	1739.9
MP_13	pp	154.2	65.7	198.6
MP_14	pp	123.3	67.5	167.6
MP_15	pp	307.7	100.9	934.8
MP_16	pp	194.9	30.6	54.6
MP_17	pp	78.4	31.5	23.1

Appendix 3

Microplastics identified with siMPle in sample number 3 (2022), DW sediment:9.69 g, Amount of sample material used for FTIR: 90%.

HH Hav 3	Polymer group	Major dimension [µm]	Minor dimension [µm]	Mass [ng]
MP_1	pe	206.4	92.2	523.5
MP_2	pe	330.9	150.2	2226.6
MP_3	pe	334.2	132.3	1746.0
MP_4	pe	611.2	157.1	4501.9
MP_5	pe	423.1	86.6	946.3
MP_6	pe	671.3	97.9	1921.7
MP_7	pe	177	94.6	473.2
MP_8	pe	51.7	31.3	15.1
MP_9	pe	391.1	172.5	3474.7
MP_10	pe	576.9	193.8	6467.3
MP_11	ps	42.4	35.4	17.4
MP_15	pp	254.2	90.3	618.6
MP_16	pp	115.6	23.7	19.3
MP_17	pp	315.5	62	362.2
MP_18	pp	134.1	23.5	22.2

Appendix 4

Microplastics identified with siMPle in sample number 4 (2021), DW sediment:9.79 g, Amount of sample material used for FTIR: 89%.

HH Hav 4	Polymer group	Major dimension [µm]	Minor dimension [µm]	Mass [ng]
MP_1	pe	171	51.6	135.7
MP_2	pe	22	10.5	0.7
MP_3	pe	245.3	125.8	1158.2
MP_4	pe	323.2	210.4	4268.0
MP_5	pe	67.6	37	27.7
MP_6	pe	272.4	142.1	1641.6
MP_7	pe	1340.5	179.1	12839.3
MP_8	pe	206.1	112.5	778.5
MP_9	pe	202.5	110.3	735.5
MP_10	pe	185.5	71.2	280.9
MP_11	pe	98.9	51.4	78.0
MP_12	pe	172.7	60.4	188.3
MP_13	pe	132.2	39.9	62.8
MP_14	pe	92	32.6	29.3
MP_15	ps	235.2	113.3	986.6
MP_16	ps	44.8	25.8	9.7
MP_19	pp	973.4	243	17153.5
MP_20	pp	22.9	10.1	0.7
MP_21	pp	427.9	140.2	2511.6

Appendix 5

Microplastics identified with siMPle in sample number 5 (2020), DW sediment:20.20 g, Amount of sample material used for FTIR: 88%.

HH Hav 5	Polymer	Major	Minor	Mass [ng]
MP_1	pe	212.5	148.6	1400.8
MP_2	pe	333.6	120.2	1438.1
MP_3	pe	57.4	28.9	14.3
MP_4	pe	61.3	24.5	11.0
MP_5	pe	308.1	167.1	2568.9
MP_6	pe	66	50.8	50.8
MP_7	pe	61.2	34.6	21.9
MP_8	pe	313.7	64.1	384.6
MP_9	pe	150.3	71	226.0
MP_10	pe	62.5	35.7	23.8
MP_11	pe	167.5	40.7	82.8
MP_12	pe	741.4	256.4	14548.7
MP_13	pe	223.3	71.4	339.8
MP_14	pe	155.1	48.7	109.7
MP_15	pe	56.9	32.5	17.9
MP_16	pe	514.8	150.7	3488.4
MP_17	pe	131.7	101.8	407.2
MP_18	pe	94.8	50.8	73.0
MP_19	pe	40.3	21	5.3
MP_20	pe	469.1	136.5	2606.9
MP_21	pe	21.1	7.3	0.3
MP_22	pe	307.1	89.7	737.0
MP_23	pe	310.2	104.4	1009.3
MP_24	pe	199.4	75.9	342.9
MP_25	pe	119.9	56.2	113.1
MP_26	ps	325.8	151.2	2433.8
MP_27	ps	246.4	149.1	1790.0
MP_28	ps	272.9	153.1	2090.9
MP_29	ps	109.8	60.3	130.5
MP_30	ps	200	121.4	962.1
MP_31	ps	283.2	102	962.7
MP_32	ps	120.7	55.9	123.0
MP_33	ps	171.2	36.2	73.4
MP_46	pp	133.6	22.8	20.7
MP_47	pp	138.9	25.2	26.4
MP_48	pp	247.8	46	156.5
MP_49	pp	1066.1	217.5	15055.6
MP_50	pp	215.9	38.5	95.7
MP_51	pp	354	26	71.4
MP_52	pp	88.7	22.1	13.0
MP_53	pp	50.9	18.2	5.0
MP_54	pp	314.2	63.9	382.5
MP_55	pp	374.1	109.3	1334.7
MP_56	pp	243.5	72.3	379.7
MP_57	pp	33.5	9.2	0.8
MP_58	pp	190.5	36.4	75.3
MP_59	pp	35.1	17.5	3.2

Appendix 6

Microplastics identified with siMPle in sample number 6 (2019), DW sediment:10.26 g, Amount of sample material used for FTIR: 89%.

HH Hav 6	Polymer group	Major dimension [µm]	Minor dimension [µm]	Mass [ng]
MP_1	pe	28.2	16.4	2.3
MP_2	pe	48.5	27	10.6
MP_3	pe	41.6	25	7.8
MP_4	pe	95.6	33.4	31.9
MP_5	pe	45	24.8	8.3
MP_6	ps	143.5	34.3	55.3
MP_9	pp	130.4	31	37.4

Appendix 7

Microplastics identified with siMPle in sample number 7 (2018), DW sediment:13.98 g, Amount of sample material used for FTIR: 80%.

HH Hav 7	Polymer group	Major dimension [µm]	Minor dimension [µm]	Mass [ng]
MP_1	pe	472.9	299.9	12692.1
MP_2	pe	185	77.5	331.2
MP_3	pe	51.7	28.3	12.4
MP_4	pe	257.9	77.3	460.6
MP_6	pp	222.7	65	281.1
MP_7	pp	135.7	78.1	246.8
MP_8	pp	272.7	69.8	396.1
MP_9	pp	279.8	101.5	859.5

Appendix 8

Microplastics identified with siMPle in sample number 8 (2017), DW sediment:13.91 g, Amount of sample material used for FTIR: 80%.

HH Hav 8	Polymer group	Major	Minor	Mass
MP_1	pe	192.8	70.9	289.4
MP_2	pe	187.5	49.1	134.9
MP_3	pe	78.4	27	17.1
MP_4	pe	126.5	42.6	68.6
MP_5	pe	208.3	42.3	111.5
MP_6	pe	187.4	21.2	25.1
MP_7	ps	47.4	35.8	19.8
MP_19	pp	237.1	65.8	306.3
MP_20	pp	263.5	29.4	67.9
MP_21	pp	303.7	186.2	3142.0
MP_22	pp	272	22.1	39.6
MP_23	pp	45	30.8	12.8
MP_24	pp	35.1	25.2	6.7
MP_25	pp	476.9	28.2	113.1

Appendix 9

Microplastics identified with siMPle in sample number 9 (2016), DW sediment:16.39 g, Amount of sample material used for FTIR: 86%.

HH Hav 9	Polymer group	Major	Minor	Mass
MP_1	pe	223.9	63.3	267.8
MP_2	pe	83.2	46.7	54.3
MP_3	pe	52.5	30.1	14.2
MP_4	pe	294.4	81.6	585.7
MP_5	pe	247.5	45.3	151.5
MP_6	pe	283.7	65	358.0
MP_7	pe	301.1	99.5	890.1
MP_8	pe	194.6	131.3	1000.3
MP_9	pe	269.9	94.6	721.1
MP_10	pe	313.1	54	272.5
MP_11	pe	192.5	39.4	89.3
MP_20	pp	387	177.6	3645.1
MP_21	pp	278.2	156.5	2032.4
MP_22	pp	286.6	39.9	136.3
MP_23	pp	35.1	18.6	3.6
MP_24	pp	183.9	34.8	66.3
MP_25	pp	590.9	136.9	3304.0
MP_26	pp	262.3	95	706.6
MP_27	pp	174.6	81.6	347.1
MP_28	pp	172.8	94	456.2
MP_29	pp	44.8	31	12.8

Appendix 10

Microplastics identified with siMPle in sample number 10 (2015), DW sediment:20.31 g, Amount of sample material used for FTIR: 84%.

HH Hav 10	Polymer group	Major dimension [µm]	Minor dimension [µm]	Mass [ng]
MP_1	pe	402.5	59.2	421.4
MP_2	pe	22	12.3	1.0
MP_3	pe	335.8	67.6	457.5
MP_7	pp	76.6	25.7	15.0
MP_8	pp	95.4	28.7	23.4
MP_9	pp	192.2	40.5	94.0

Appendix 11

Microplastics identified with siMPle in sample number 11 (2014), DW sediment:20.31 g, Amount of sample material used for FTIR: 89%.

HH Hav 11	Polymer group	Major dimension [µm]	Minor dimension [µm]	Mass [ng]
MP_1	pa	130.2	20.4	19.4
MP_2	pe	333.9	56.7	320.9
MP_3	pe	382.4	171.5	3358.1
MP_4	pe	61.2	25.8	12.2
MP_20	pp	267.6	99.9	796.8
MP_21	pp	488.7	95.9	1341.8
MP_22	pp	760.4	29.8	201.3
MP_23	pp	271.4	71.7	416.0
MP_24	pp	161.1	94.4	428.8
MP_25	pp	211.8	19.6	24.4
MP_26	pp	138.5	58.9	143.6
MP_27	pp	375.8	50.1	281.7

Appendix 12

Microplastics identified with siMPle in sample number 12 (2013), DW sediment:19.28 g, Amount of sample material used for FTIR: 82%.

HH Hav 12	Polymer group	Major dimension [µm]	Minor dimension [µm]	Mass [ng]
MP_1	pe	392.6	99.7	1164.2
MP_2	pe	229.9	30.2	62.4
MP_3	pe	273.7	122	1215.9
MP_4	pe	299.5	57.1	291.4
MP_5	pe	109	42.4	58.5
MP_6	pe	180.6	40.9	90.4
MP_7	pe	81.8	30.6	22.9
MP_14	pp	58.7	17.7	5.5
MP_15	pp	201.5	60.8	222.2
MP_16	pp	458.7	291.6	11636.3
MP_17	pp	742.1	174	6707.6
MP_18	pp	307.6	82.3	621.3
MP_19	pp	56.9	35.2	21.0
MP_20	pp	311.6	40	149.1
MP_21	pp	370.8	76.8	652.0
MP_22	pp	335	47.6	226.5
MP_23	pp	97.1	18.6	10.1
MP_24	pp	183.4	22.9	28.7
MP_25	pp	166.4	45.1	101.2

Appendix 13

Microplastics identified with siMPle in sample number 13 (2012), DW sediment:15.66 g, Amount of sample material used for FTIR: 79%.

HH Hav 13*	Polymer group	Major dimension [µm]	Minor dimension [µm]	Mass [ng]
MP_1	pe	39	24.7	7.1
MP_2	pe	238.7	90.2	579.5
MP_3	pe	100.3	41.5	51.5
MP_4	pe	98.7	63.6	119.1
MP_5	pe	76.5	28.7	18.8
MP_6	pe	282.8	59.9	303.1
MP_7	pe	73.5	29.9	19.6
MP_8	pe	73.1	27.4	16.4
MP_9	pe	153.3	53.8	132.3
MP_10	pe	222.9	32.3	69.5
MP_11	pe	104.9	29.4	27.0
MP_12	pe	128.9	51.4	101.7
MP_13	pe	172.8	65.3	219.9
MP_14	pe	181	96	497.5
MP_15	pe	56.9	27.1	12.4
MP_20	pp	58.7	21.7	8.2
MP_21	pp	275.5	103.9	887.3
MP_22	pp	301.2	63.4	361.6
MP_23	pp	181.3	51.8	145.4
MP_24	pp	299.5	44.6	178.0
MP_25	pp	148.3	28	34.8
MP_26	pp	267.3	86.2	592.2
MP_27	pp	51.7	21.6	7.2
MP_28	pp	330.2	34.8	119.1

Appendix 14

Microplastics identified with siMPle in sample number 14 (2011), DW sediment:20.45 g, Amount of sample material used for FTIR: 93%.

HH Hav 14	Polymer group	Major dimension [µm]	Minor dimension [µm]	Mass [ng]
MP_1	pe	319.9	179.1	3060.5
MP_2	pe	53.6	35.2	19.8
MP_3	pe	106.4	30.4	29.4
MP_4	pe	304.6	56.7	291.7
MP_5	pe	150.7	82.5	306.5
MP_6	pe	151.2	42.3	80.7
MP_7	pe	247.7	49.5	180.8
MP_8	ps	83.2	38.4	40.1
MP_12	pp	537.4	56	503.8
MP_13	pp	271.7	62.5	316.9
MP_14	pp	121.3	17.1	10.6
MP_15	pp	122.9	26	24.8
MP_16	pp	216.5	47	142.5
MP_17	pp	51.3	20.3	6.3
MP_18	pp	244.6	32.7	78.3
MP_19	pp	202.4	42.1	106.8
MP_20	pp	30.1	20.5	3.8

Appendix 15

Microplastics identified with siMPle in sample number 15 (2010), DW sediment: 16.87 g, Amount of sample material used for FTIR: 90%.

HH Hav 15	Polymer group	Major dimension [µm]	Minor dimension [µm]	Mass [ng]
MP_1	pe	262.5	148.1	1717.4
MP_2	pe	273.1	85.6	597.4
MP_3	pe	182.7	43.8	104.8
MP_4	pe	93.3	40	44.6
MP_6	pp	473.7	132	2461.9
MP_7	pp	147.1	51.8	118.0
MP_8	pp	142.9	61.7	162.5

Appendix 16

Microplastics identified with siMPle in sample number 16 (2009), DW sediment:17.04 g, Amount of sample material used for FTIR: 90%.

HH Hav 16	Polymer group	Major dimension [µm]	Minor dimension [µm]	Mass [ng]
MP_1	pe	82	41.8	42.8
MP_2	pe	269.1	110.5	980.7
MP_9	pp	707.6	35.2	261.9
MP_10	pp	204	13	10.3
MP_11	pp	44.4	13	2.2
MP_12	pp	81.4	40.2	39.3
MP_13	pp	163.8	43.5	92.5
MP_14	pp	28.2	12.3	1.3
MP_15	pp	226.8	55.5	208.7
MP_16	pp	279.3	86.6	625.1
MP_17	pp	61.3	20.1	7.4
MP_18	pp	96.1	39.3	44.2
MP_19	pp	133.4	41.9	69.8
MP_20	pp	28.8	20	3.5